

LOW-RANK COAL RESEARCH
SEMIANNUAL REPORT
JANUARY, 1992 - JUNE, 1992
COOPERATIVE AGREEMENT DE-FC21-86MC10637

For
U.S. Department of Energy
Morgantown Energy Technology Center
Morgantown, West Virginia

By
University of North Dakota
Energy and Environmental Research Center
Grand Forks, North Dakota

1.0 TABLE OF CONTECTS

TABLE OF CONTENTS

1.0 TABLE OF CONTENTS

2.0 CONTROL TECHNOLOGY AND COAL PREPARATION RESEARCH

- 2.1 Flue Gas Cleanup
- 2.2 Waste Management
- 2.3 Regional Energy Policy Program for the Northern Great Plains
- 2.4 Hot-Gas Cleanup

3.0 ADVANCED RESEARCH AND TECHNOLOGY DEVELOPMENT

- 3.1 Turbine Combustion Phenomena
- 3.2 Combustion Inorganic Transformation
- 3.3 (Combined with Section 3.2 in Year 4)
- 3.4 Liquefaction Reactivity of Low-Rank Coals
- 3.5 Gasification Ash and Slag Characterization
- 3.6 Coal Science

4.0 COMBUSTION RESEARCH

- 4.1 Atmospheric Fluidized-Bed Combustion
- 4.2 Beneficiation of Low-Rank Coals
- 4.3 Combustion Characterization of Low-Rank Coal Fuels
(COMPLETED 10-31-90)
- 4.4 Diesel Utilization of Low-Rank Coals
(COMPLETED 12-31-90)
- 4.5 Produce and Characterize HWD Fuels for Heat Engine Applications
(COMPLETED 10-31-90)
- 4.6 Nitrous Oxide Emissions
- 4.7 Pressurized Fluidized-Bed Combustion

5.0 LIQUEFACTION RESEARCH

- 5.1 Low-Rank Coal Direct Liquefaction

6.0 GASIFICATION RESEARCH

- 6.1 Production of Hydrogen and By-Products from Coal
- 6.2 Sulfur Forms in Coal

2.0 CONTROL TECHNOLOGY AND COAL PREPARATION RESEARCH

2.1 Flue Gas Cleanup

FLUE GAS CLEANUP

Semiannual Technical Progress Report
for the Period January 1, 1992 - June 30, 1992

by

Stanley J. Miller, Research Supervisor
Marlys K. Heidt, Research Engineer
Dennis L. Laudal, Research Engineer
Greg F. Weber, Research Supervisor

Energy and Environmental Research Center
University of North Dakota
P.O. Box 8213, University Station
Grand Forks, ND 58202-8213

Technical Monitor: Perry D. Bergman

for

U.S. Department of Energy
Pittsburgh Energy Technology Center
626 Cochran Mill Road
Pittsburgh, PA 15236-0940

July 1992

MASTER

DISTRIBUTION OF THIS DOCUMENT IS UNLIMITED

Work Performed Under Cooperative Agreement No. DE-FC21-86MC10637

TABLE OF CONTENTS

	Page
LIST OF FIGURES	ii
LIST OF TABLES	iii
1.0 INTRODUCTION	1
2.0 BACKGROUND	1
3.0 GOALS AND OBJECTIVES	3
4.0 ACCOMPLISHMENTS	4
4.1 Fine-Particulate Control	4
4.1.1 Review of Previous Cohesive Measurements and Reentrainment Experiments	4
4.1.2 Pore-Bridging and Reentrainment Tests	5
4.1.3 Horizontal Reentrainment Tests	11
4.1.4 Conclusions from the Fine-Particulate Control Work	19
4.2 Impact of Coal Combustion on Atmospheric Visibility	19
4.2.1 Causes of Visibility Impairment	19
4.2.2 Source Contribution to Visibility Impairment	22
4.2.3 Atmospheric Chemistry	25
4.2.4 Coal Combustion and Visibility	26
4.2.5 Effect of Reduced Emissions on Atmospheric Visibility	27
4.2.6 Summary of Literature Review on Atmospheric Visibility	30
4.2.7 Summary of Selected Literature Sources	31
5.0 REFERENCES	45

LIST OF FIGURES

<u>Figure</u>		<u>Page</u>
1	Effect of pore size on maximum pore-bridging velocity for screen tests with baseline and conditioned Monticello fly ash	7
2	Maximum pore-bridging velocity for the 150- μm screen as a function of tensile strength	8
3	Effect of face velocity on K_2 for screen tests with baseline and conditioned Monticello fly ash	9
4	Correlation between K_2 and packed or aerated porosity for 13 μm MMD fly ash	10
5	Correlation between K_2 and aerated or packed porosity for 13 μm and 4.5 μm MMD fly ash	10
6	Horizontal reentrainment test system	12
7	Reentrainment results with ash layer smoothed over with a knife edge	13
8	Reentrainment results for baseline Monticello fly ash with flow gate in front of ash layer	14
9	Reentrainment results for conditioned Monticello fly ash with flow gate in front of ash layer	14
10	Reentrainment results for baseline Big Brown fly ash with flow gate in front of ash layer	15
11	Reentrainment results for conditioned Big Brown fly ash with flow gate in front of ash layer	15
12	Comparison of reentrainment between baseline and conditioned Monticello fly ash with flow gate in front of ash layer	16
13	Comparison of reentrainment between baseline and conditioned Big Brown fly ash with flow gate in front of ash layer	16
14	Comparison of reentrainment between baseline and conditioned Monticello fly ash with flow gate over the middle of ash layer	17
15	Comparison of reentrainment between baseline and conditioned Big Brown fly ash with flow gate over the middle of ash layer	18

LIST OF TABLES

<u>Table</u>		<u>Page</u>
1	Fine-Particulate Contribution to the Extinction Coefficient for the Denver Wintertime Aerosol	22
2	Natural Background Levels of Atmospheric Aerosols	23

FLUE GAS CLEANUP

1.0 INTRODUCTION

From April 1983 through March 1988, the focus of the Cooperative Agreement SO_x/NO_x Control project was investigation of dry sorbent injection for SO_x control and methods of enhancing SO_x sorbent reactivity/utilization. The primary emphasis was furnace injection of calcium-based sorbents with some experiments evaluating back-end humidification (1,2). In April 1988, the emphasis of the project was changed to advanced NO_x control with application to new and existing utility systems, as well as control of NO_x emissions from industrial-scale combustors. Specific activities for the period April 1988 through June 1989 focused on the bench-scale evaluation of a catalyst-coated woven fabric filter for simultaneous NO_x and particulate control (3). In June 1989, the project name was changed from SO_x/NO_x Control to Flue Gas Cleanup, and the scope of project activities was expanded to include tasks supporting bench-scale work in the fine-particulate control area. Work in the fine-particulate control area was included as a separate project within the Cooperative Agreement from April 1983 through March 1988 and was also funded as a result of a competitive DOE award during the period May 1988 through December 1989.

In March 1990, the Energy and Environmental Research Center (EERC) was notified that a proposal, in response to RFP DE-RP22-89PC89801 entitled "Development of Advanced NO_x Control Concepts for Coal-Fired Utility Boilers," was selected for funding. Therefore, catalytic fabric filter development activities have been deleted from the Cooperative Agreement Flue Gas Cleanup project.

At the request of Department of Energy-Pittsburgh Energy Technology Center (DOE-PETC), a task was added this year (July 1, 1991 through June 30, 1992) to assess the effect of coal combustion on visibility impairment in the atmosphere. Therefore, the Flue Gas Cleanup project is currently focusing on two areas: 1) bench-scale efforts to further investigate the relationships between fine-particle emissions from fabric filters and the cohesive properties of fly ash, and 2) investigation of the impact of coal combustion on atmospheric visibility.

This report documents the work for the Flue Gas Cleanup project for the period January 1 through June 30, 1992.

2.0 BACKGROUND

Present New Source Performance Standards for utility coal-fired boilers limit particulate emissions to 0.03 lb/million Btu and require 20% or lower opacity. The control device removal efficiency required to meet this standard varies from about 99% to 99.9%, depending on the heating value and ash content of the coal. Electrostatic precipitators or fabric filters are the technologies that have most often been employed to meet the current standard. Although the best proven control technology for fine-particulate matter appears to be fabric filtration if it is properly designed, both of these technologies have been successful, in most cases, in meeting the current standard. However, the removal efficiency of both electrostatic precipitators

and baghouses is significantly reduced for fine particles less than 2 μm . Emissions of fine particles are of concern because these particles are likely to be deposited in the lower respiratory system through normal breathing. The problem is further compounded because hazardous trace elements such as selenium and arsenic are known to be concentrated on such fine particles. Control device removal efficiency is lowest for respirable particles, so a situation exists where the most hazardous particles from coal combustion are collected with the lowest removal efficiency. In addition to causing adverse health effects, fine-particle emissions have an impact on atmospheric visibility. Particles which are the most efficient at scattering light (0.1-2 μm) do not readily settle out of the atmosphere and are subject to long-range transport. When present in sufficient concentrations, these fine particles will cause serious visibility impairment. Therefore, the emission of fine particles is an issue because of potential adverse health effects and visibility impairment in the atmosphere.

Previous results at the EERC show that fine-respirable-particulate emissions can be reduced by up to 4 orders of magnitude by injecting small amounts of ammonia and SO_3 upstream of a baghouse (4-15). This corresponds to an increase in collection efficiency, for some difficult-to-collect ashes, from 90% to 99.999%. Emissions in some tests are less than ambient particulate levels in the atmosphere. Along with reduced particulate emissions, baghouse pressure drop is also reduced, making the process more economical. With some coals, pressure drop was reduced by 75%. Conditioning would add about 9% to the cost of operating a conventional reverse-gas baghouse, but this cost could be more than recovered if pressure drop and/or size of the baghouse is reduced.

The conditioning agents make the ash particles more cohesive which reduces the seepage of dust through the fabric and facilitates the bridging of pinholes, preventing direct particle penetration. At the same time, a more porous dust cake is formed, which results in reduced baghouse pressure drop. A review of penetration mechanisms shows that there is a theoretical basis for lower emissions with increased bulk cohesive strength. Pressure drop reduction as a result of conditioning is attributed to an increase in dust cake porosity as theoretical and empirical models predict. To further develop this technology the cohesive characteristics of fly ash must be quantified and related to fabric filter performance. There is a need to test existing methods and select or develop reliable methods to measure cohesive properties of fly ash. Further, the measured cohesive properties should be correlated with other ash properties to understand which ash properties control cohesive strength and to help understand how ash properties affect fine-particle emissions from fabric filters.

In 1977, Congress added Section 169A to the Clean Air Act (CAA) which established as a national goal "the prevention of any future, and the remedying of any existing, impairment of visibility in mandatory Class I Federal areas which impairment results from man-made air pollution." The Environmental Protection Agency (EPA) defines "visibility impairment" as "any humanly perceptible change in visibility (visible range, contrast, coloration) from that which would have existed under natural conditions." The EPA has identified two types of air pollution that impair or reduce visibility. The first is single-source impairment defined by the EPA as smoke, dust, colored gas plumes, or layered haze emitted from stacks that obscure the sky or horizon, and are relatable in a single source or a small group of sources.

The second type is regional haze which is widespread, regionally homogeneous haze from a multitude of sources, and impairs visibility in every direction over a large area. The EPA has used a phased approach to implement the visibility program. Phase I of the program requires control of impairment that can be traced to a single existing stationary facility or small group of existing stationary facilities. Section 169B was added to the CAA in 1990 to determine the need for expansion of the visibility protection program. It provides funding for continued research on visibility in Class I federal areas including: 1) expansion of current visibility impairment monitoring, 2) assessments of current sources of visibility impairment using regional air quality models, and 3) studies on atmospheric chemistry and the physics of visibility. Section 169B also calls for the creation of Visibility Transport Regions consisting of one or more states which, because of interstate pollution, contribute significantly to visibility impairment in Class I areas. After the creation of Visibility Transport Regions, Visibility Transport Commissions (VTCs) (whose members include the Governors of the affected states) will be formed to address the establishment of clean air corridors, restrictions on new construction, and the development of long-range strategies for remedying regional haze.

Visibility has been the focus of a significant amount of research for over a decade. However, attempts to accurately identify the contributions of various sources to visibility impairment have been hampered by the limitations of air quality models and the lack of understanding of the complex physical and chemical processes that govern the formation of secondary aerosols in the atmosphere.

3.0 GOALS AND OBJECTIVES

The general objective of the DOE Flue Gas Cleanup Program, under the direction of the PETC, is to promote the widespread use of coal. This is to be accomplished by providing the technology necessary for utilization of coal in an environmentally and economically acceptable manner. The program addresses the reduction of acid rain precursor emissions as well as development of technologies with the potential to meet more stringent emissions control requirements for SO₂, NO_x, and particulate matter.

For this current project year, only the fine-particulate control area of the DOE Flue Gas Cleanup Program is addressed. Specific activities involve the development of methods to measure the cohesive strength and reentrainment potential of fly ashes relative to fine-particle emissions from fabric filters and an assessment of the impact of coal combustion on atmospheric visibility. The general objective of the fine-particulate control effort is to develop methods to help characterize, control, and model fine-particulate emissions from a fabric filter. Characterization efforts include the development of methods to measure the cohesive strength and reentrainment potential of fly ashes. Control and modeling efforts involve relating these parameters to the level of fine-particle emissions from fabric filters. Specific goals this year include the following:

1. Correlate measured cohesive strength with other ash properties such as particle size, particle shape, surface area, porosity, and ash chemistry.

2. Measure the reentrainment potential of ash from the surface of a fly ash filter cake or bulk fly ash and relate it to the measured cohesive strength.
3. Perform a literature review to determine the status of the visibility issue as it relates to coal combustion. Based on the information collected, prepare a multiyear work plan for the visibility activities within the Flue Gas Cleanup project.
4. Evaluate the potential for applying new particle measurement methods to atmospheric aerosols, relating the results to direct visibility measurements.

4.0 ACCOMPLISHMENTS

4.1 Fine-Particulate Control

4.1.1 Review of Previous Cohesive Measurements and Reentrainment Experiments

The bench-scale efforts this year (July 1, 1991 through June 30, 1992) were a continuation of the Fine-Particulate Control work completed last year (July 1, 1990 through June 30, 1991). Recent results were reported in the last two semiannual reports (15,16). The primary focus of the work has been to develop methods to measure the cohesive properties of fly ash and relate these properties to filtration behavior. This information should lead to a better understanding of how fly ash properties affect fine-particle emissions from fabric filters and how conditioning the fly ash improves fabric filter performance. It is expected that superior fine-particulate control can be achieved at a reduced cost compared to existing technologies, either by employing flue gas conditioning or by other design optimization methods.

Quantification of the cohesive character of fly ash for modeling fabric filter performance is analagous to the measurement of fly ash resistivity to model electrostatic precipitator (ESP) performance. Resistivity measurement provides a basis to design ESPs for a target level of collection efficiency based on a property of the dust. An equivalent measurement of the cohesive character of fly ash could provide a basis for design of fabric filters in terms of fabric selection and air-to-cloth ratio to achieve a target collection efficiency and pressure drop for a given dust. The availability of such a measurement would facilitate optimization of fabric filters to provide the highest fine-particle collection efficiency at the lowest cost. However, there is presently no consensus as to what characteristics of the fly ash should be measured or is there an accepted protocol for such measurements as tensile strength and porosity. Data suggest that both tensile strength and porosity measurements provide critical information that can be used to predict collection efficiency and pressure drop, but both approaches need further evaluation and development.

During the last two years, initial measurements were conducted with a Cohetester and a Powder Characteristics Tester. These two instruments directly measure the tensile strength and porosity of fine powders, respectively. A description of these instruments, along with the test procedures, was given in the July 1989-June 1990 annual report (14).

One of the effects of conditioning is an increase in fly ash tensile strength at constant porosity or an increase in porosity at constant tensile strength. When tensile strength was plotted as a function of porosity, the primary effect of conditioning was a shift in the curve upward (higher tensile strength) and to the right (higher porosity). Initial results also showed that the tensile strength measurements may be affected by the ambient relative humidity. Subsequent tensile strength measurements were conducted to evaluate the effect of relative humidity by exposing the samples to carefully controlled humidity conditions. Results showed that the tensile strength of baseline fly ashes were not as sensitive to relative humidity, as were the conditioned fly ashes. This indicates that there is an interaction between conditioning and relative humidity. From the measurements conducted to date, it appears that tensile strength is an excellent method to quantify the cohesive character of fly ash, and that tensile strength correlates with filtration behavior such as pore-bridging ability. However, measurement of fly ash tensile strength is still under development and is not an accepted or standard method.

Porosity and tensile strength are measures of the cohesive character of a dust, but, by themselves, do not provide any predictive indication of filtration behavior unless they can be directly correlated with filtration performance data. Previous data indicated that differences in collection efficiency in a fabric filter with different dusts could be linked to the pore-bridging ability and reentrainment potential of the dust. The fabric filter data also showed that differences in pressure drop with different dusts are tied to the specific dust cake resistance coefficient, K_2 , of the dusts. Therefore, if pore-bridging ability, reentrainment potential, and K_2 can be measured directly in the laboratory, and, if these measurements correlate with the tensile strength and porosity measurements, there is a basis for prediction of fabric filter performance from cohesive characteristics.

To better understand filtration performance, work was conducted to look at the reentrainment properties and the pore-bridging behavior of fly ash. Measurement of pore bridging and the reentrainment of conditioned and baseline fly ash was conducted as a function of pore size and face velocity. Pore-bridging and reentrainment tests showed that conditioned ash is more effective at bridging pores over the entire velocity range tested (15). An explanation is that the particle-to-particle binding forces must be greater with conditioning. However, pore-bridging ability apparently cannot be predicted on the basis of tensile strength alone because superior bridging was also achieved at lower tensile strengths. The exact physical parameters that predict pore-bridging ability, based on last year's experiments were not clear. While significant new data were added to help predict filter performance on the basis of dust properties, more work was needed. Therefore, further work was conducted this project year by adding the variables of particle size and relative humidity to pore-bridging and reentrainment tests.

4.1.2 Pore-Bridging and Reentrainment Tests

Initial tests were conducted with a reentrainment cell in which an ash layer was placed manually on a horizontal screen without air flow (14). Air was introduced downward through the layer, and particulate emissions monitored as the face velocity of air through the ash layer was slowly increased. Results showed that the velocity at which significant reentrainment occurred

depended on pore size; whether conditioned or baseline fly ash was used; and, to a lesser extent, on the level of packing of the ash layer. However, one drawback to this approach is that the ash layer was not formed from dust cake buildup during a filtration process and may not have been indicative of dust cake structure that occurs in fabric filtration. Therefore, last year, pore-bridging and reentrainment tests were conducted under actual filtration conditions. The experimental system consisted of a filter holder containing a 0.42-ft² filter sample and a dry-powder disperser to introduce the fly ash into a carrier gas upstream of the filter. The system was originally designed so that the filter could be operated at 300°F and ammonia and SO₃ could be injected upstream of the filter. Tests last year, however, were conducted at ambient temperature and without conditioning agents, although modifications were made so that relative humidity could be precisely controlled.

Pore-bridging experiments were conducted to investigate the effect of particle size and relative humidity on the pore-bridging ability of baseline and conditioned Monticello fly ash. The carrier gas was dry compressed air, with part of the carrier gas diverted through a controlled temperature water bath prior to the dry-powder disperser and filter holder. A humidity sensor was placed in the filter holder to continuously monitor the relative humidity of the air passing through the filter. By changing the fraction of gas that passed through the water bath and the water temperature, the relative humidity at the filter could easily be controlled. At the start of each test, the airflow rate was set, and background particulate levels of the clean carrier gas were measured. As expected, background particulate levels were very low and not a source of interference. Dust was then fed for a period of 35 minutes, while particulate emissions and pressure drop were recorded as a function of time. Respirable-mass-particulate emissions were measured with an aerodynamic particle sizer (APS), and submicron particles were measured with a condensation nucleus counter (CNC). Inspection of both the clean and dirty sides of the screens through sight ports gave visual proof of complete pore bridging or the formation of pinholes. A constant volumetric dust feed rate was used for all of the tests, based on a feeder piston speed of 100 mm/hr, which corresponds to about 65 grams of baseline dust and 47 grams of the conditioned dust. The weight of dust remaining on the filter at the end of each test was determined allowing calculation of K₂ values in cases where a sufficient dust cake remained intact on the filter and where pinholes were not present in significant quantities.

Pore-bridging was evaluated as a function of particle size, pore size, gas velocity and relative humidity. The particle-size effect was evaluated in the current project year by conducting additional pore-bridging tests at 15% and 50% relative humidity with the size-fractionated (4.5 μm) baseline and conditioned Monticello fly ashes. Gas velocity ranged from 1 to 8 ft/min and pore size ranged from 20 to 300 μm. Only enough tests were conducted to establish the maximum velocity at which complete bridging occurred for a given pore size rather than to complete a full matrix with these variables. For example, if results showed that complete bridging occurred with a 150-μm screen, there would be no reason to test smaller screen sizes at the same velocity. Similarly, if bridging did not occur for a given velocity with a 150-μm screen, there would be no reason to conduct a test at the same velocity with the larger 300-μm screen.

The effect of conditioning and relative humidity on the pore-bridging ability of the dusts from the screen tests is shown in Figure 1. No

improvement in pore-bridging ability was seen with the increase in relative humidity for the baseline ash. However, as Figure 1 shows, an increase in relative humidity had a dramatic effect on pore-bridging ability of the conditioned Monticello fly ash. Looking at the 150- μm screen data in Figure 1 reveals that the greatest shift in the bridging velocity vs. pore size curve was between the conditioned ash at 15% and 50% relative humidity, which is consistent with previous tensile strength data (15,16). From these observations, a good predictor of pore-bridging ability appears to be tensile strength. The maximum bridging velocity, as a function of tensile strength for the 150- μm screen, is shown in Figure 2. In Figure 2, the curve on the left was obtained from the tensile strength vs. porosity curves (extrapolating where necessary) using the dust cake porosity, which was inferred from K_2 measurements. The curve on the right was obtained using the tensile strength at the maximum compaction pressure (lowest porosity). Although the curve on the left would appear to be more valid, uncertainty is introduced because extrapolation is required to obtain the tensile strength for some cake porosities. Therefore, it may be preferable to predict pore bridging from the tensile strength data at maximum compaction pressure since it is known with

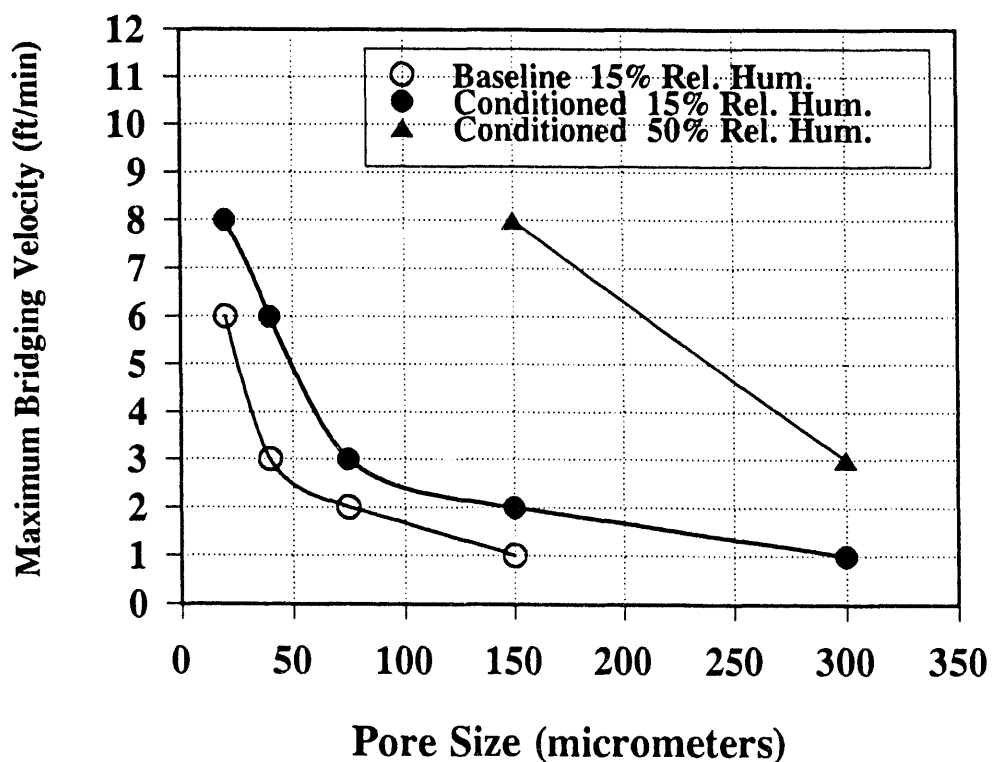


Figure 1. Effect of pore size on maximum pore-bridging velocity for screen tests with baseline and conditioned Monticello fly ash.

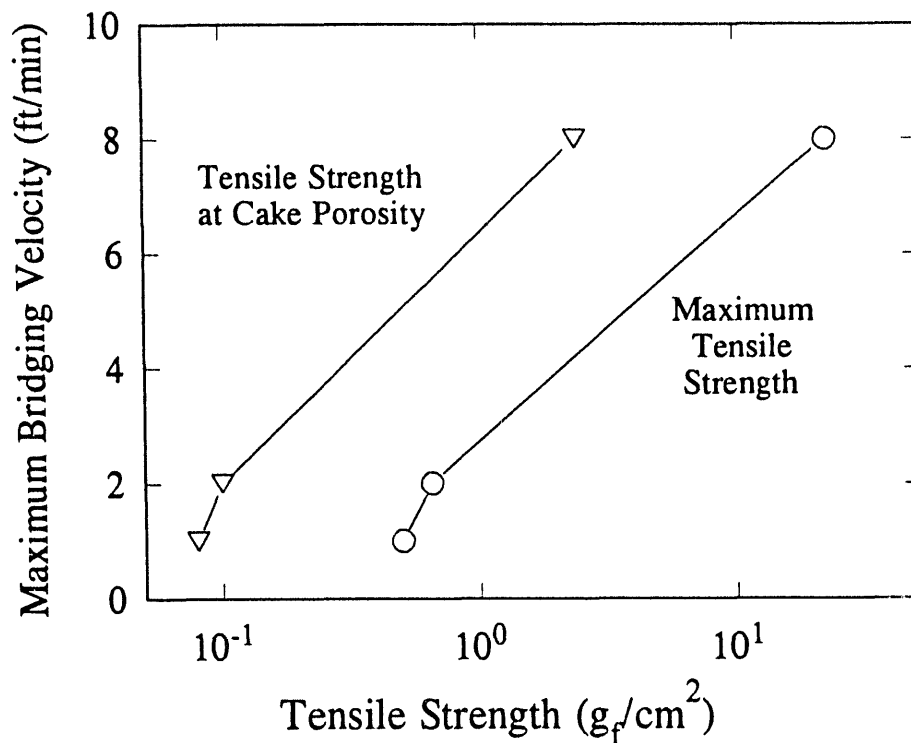


Figure 2. Maximum pore-bridging velocity for the 150- μm screen as a function of tensile strength.

greater certainty. Again, much more data are needed to further evaluate and refine this correlation. Plans are to continue the development of this correlation.

Figure 3 presents the effects of conditioning, particle size, and relative humidity on K_2 for the screen tests. Results show that the smaller 4.5- μm dusts had higher K_2 values, as expected. Pressure drop models, such as Carman-Kozeny, which exhibit an inverse square relationship between K_2 and particle size, indicate that K_2 for a 4.5- μm dust should be about 8 times greater than the K_2 for a 13- μm dust at constant porosity. However, a more porous cake is typically formed with a smaller particle size, partially offsetting the particle-size effect. This explains why the K_2 values of the 4.5- μm dusts (shown in Figure 3) were only from about 1.2 to 2.5 times greater than the corresponding 13- μm dusts.

The results shown in Figure 3 can be related to the cohesive characteristics of the fly ashes by comparing the data with aerated and packed porosity measurements (Figures 4 and 5). Figure 4 indicates that both the aerated and packed porosity measurements correlate closely with K_2 for a constant velocity and for dusts with approximately the same particle-size distribution. It is evident, however, that the K_2 measurements can be significantly influenced by gas velocity which, therefore, must be included in

any attempt to predict K_2 on the basis of porosity measurements. Figure 5 shows the relationship between porosity and K_2 at constant velocity, but with two different particle sizes. These data indicate that porosity measurements can be used as a basis to predict K_2 , but only if velocity and particle size are also incorporated into a model. The three variables, along with possible interactions among them, suggest that much more work is needed to develop a predictive model for K_2 .

Another aspect of filter performance is bag cleanability, which is also dependent on the cohesive properties of the dust. The correlations imply that, for dusts of similar particle-size distributions, the dusts with the highest tensile strengths and porosities will form dust cakes with the lowest K_2 values. However, this is only true if the residual dust cake weight does not increase. If the tensile strength is high, bags may not be easily cleaned and high dust cake weights could result. Nevertheless, the measured tensile strength and porosity of a dust can be used to predict qualitatively pore-bridging ability and dust cake resistance, which are the main indicators of filter performance.

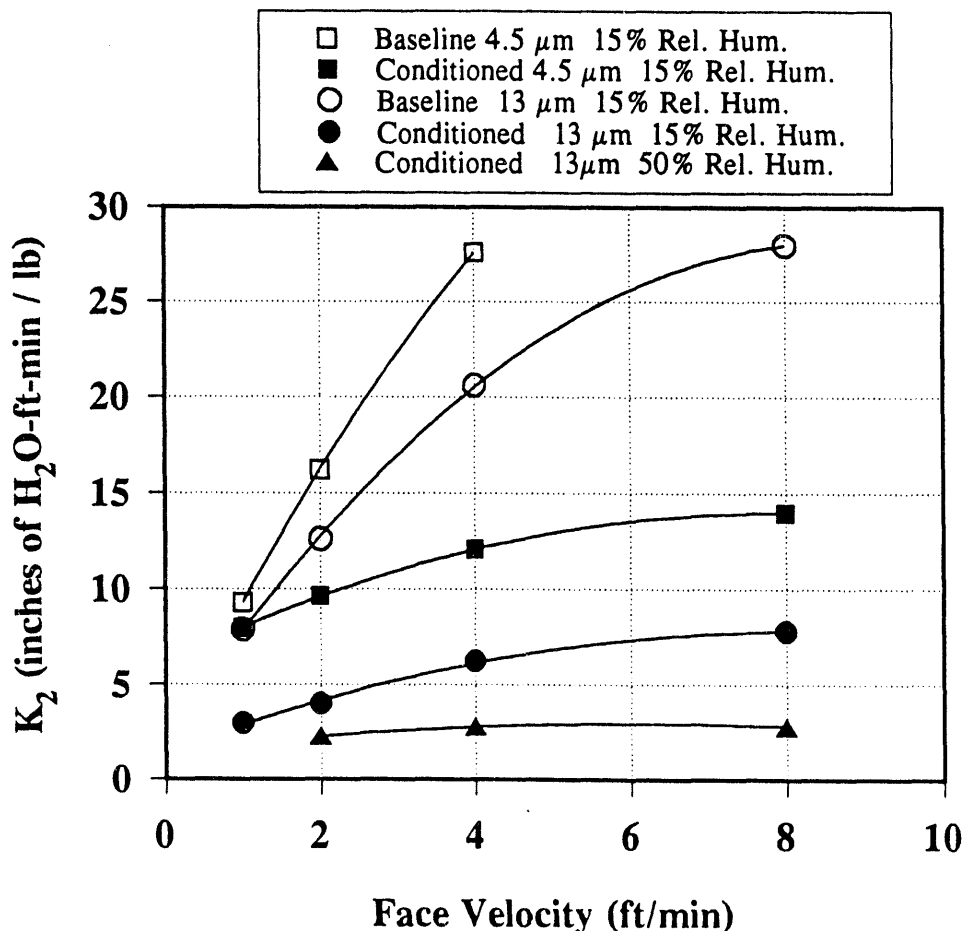


Figure 3. Effect of face velocity on K_2 for screen tests with baseline and conditioned Monticello fly ash.

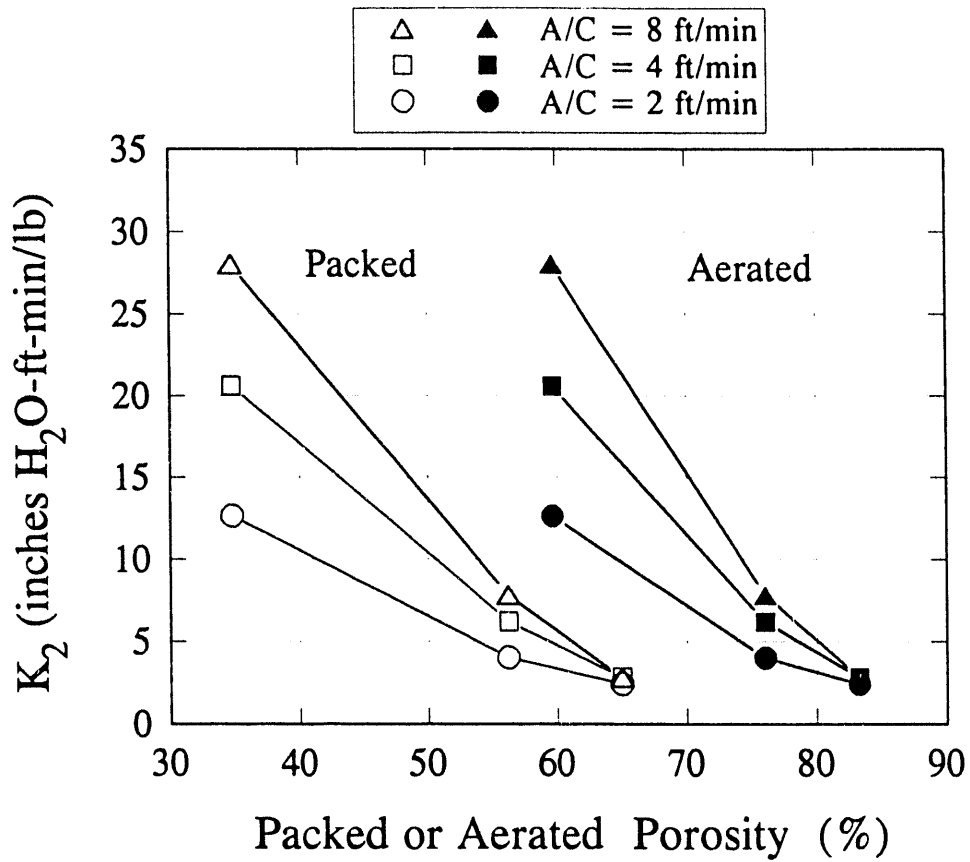


Figure 4. Correlation between K_2 and packed or aerated porosity for 13- μm MMD fly ash.

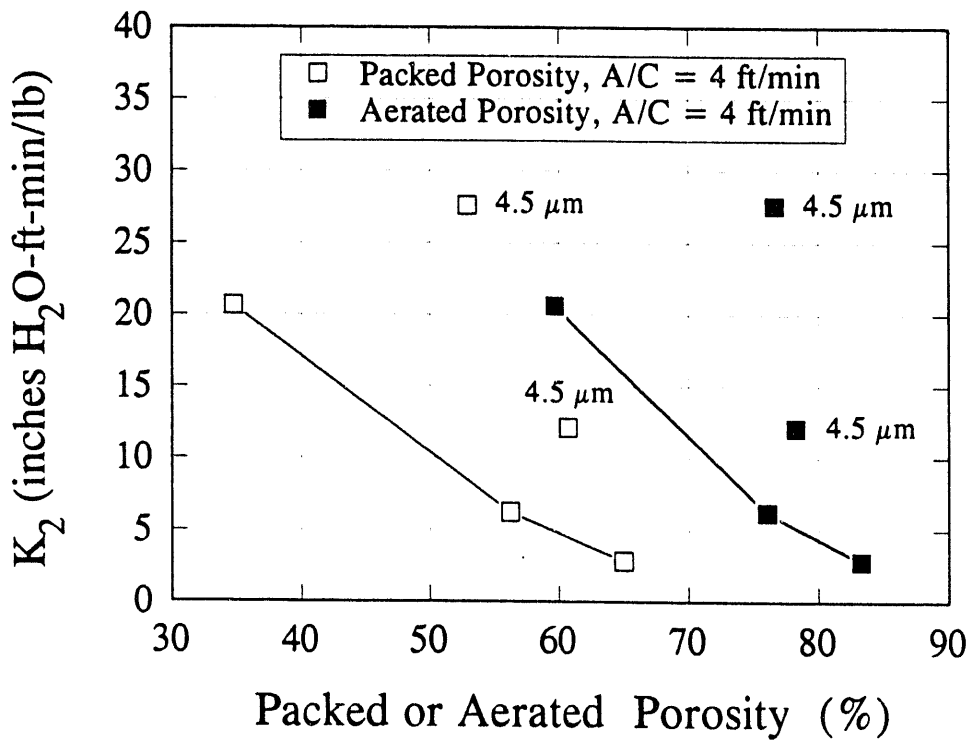


Figure 5. Correlation between K_2 and aerated or packed porosity for 13- μm and 4.5- μm MMD fly ash.

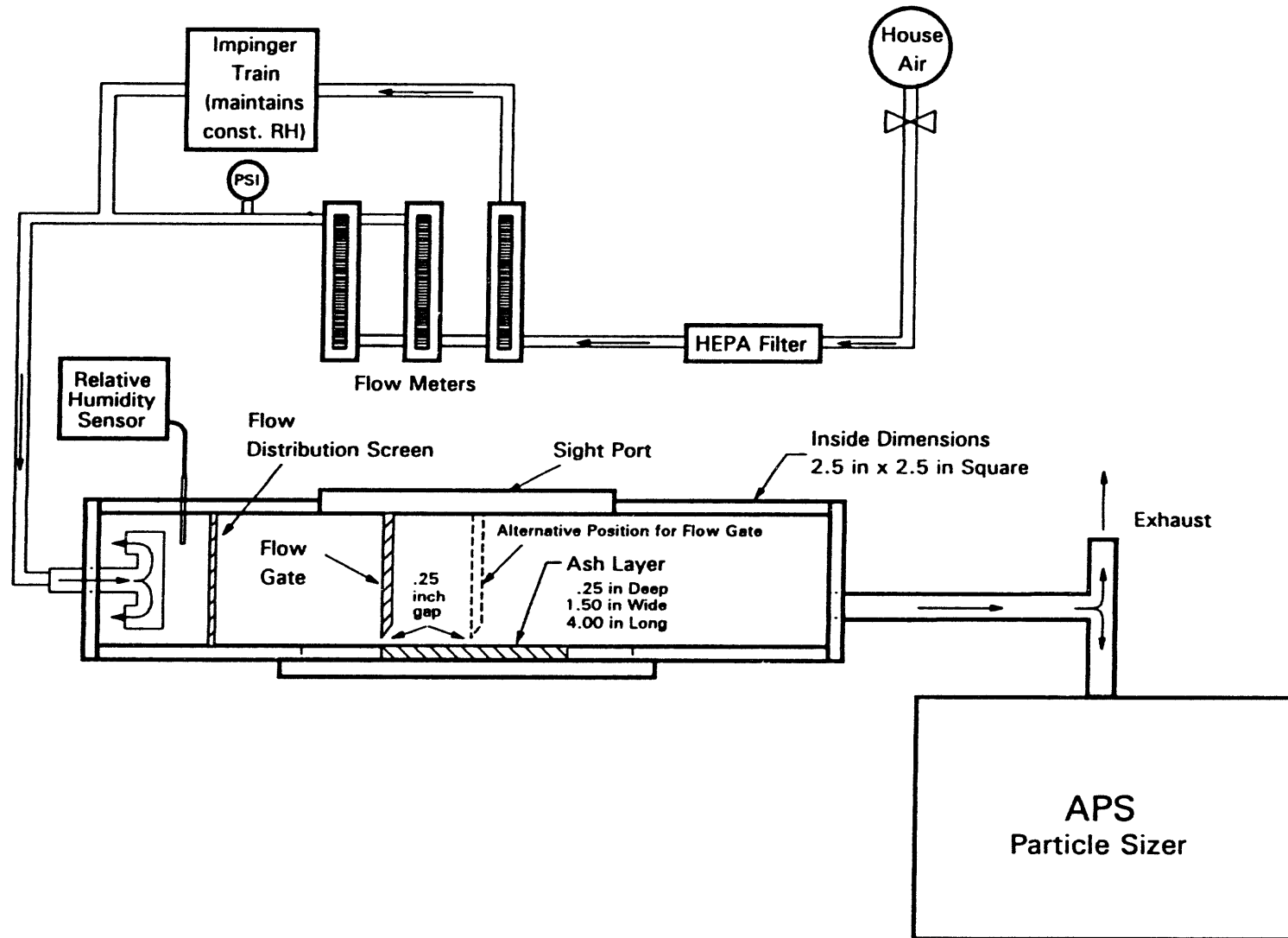
4.1.3 Horizontal Reentrainment Tests

Reentrainment tests were also conducted with a bench-scale test system designed to investigate particle reentrainment with flow parallel to the dust surface, as shown in Figure 6. Initial tests, in which the flow velocity across the dust layer was determined by the cross-sectional area of the 2.5-in by 2.5-in square duct, showed that detectable reentrainment did not occur for duct velocities smaller than 5 ft/s and the flowmeters and tubing could not handle higher flow rates. Therefore, to achieve higher velocities across the ash up to 50 ft/s, a gate was installed at either the beginning or middle of the ash layer, as shown in Figure 6. This configuration enabled testing over velocities for which significant reentrainment occurred.

For the initial tests with the gate configuration, the dust was placed in the bottom of a flow channel with a recessed ash holder, and the surface of the ash was smoothed with a knife edge so that the ash layer was flush with the wall of the flow channel. To determine reentrainment, respirable mass measurements were taken every two minutes up to a total test time of 8 minutes for a given velocity. After eight minutes, the velocity was increased and respirable mass measurements were taken every two minutes. The velocity typically ranged from 5 ft/s when initial reentrainment was detected, up to 35 ft/s when significant reentrainment occurred. Results showed a velocity of at least 5 ft/s was required to induce reentrainment (see Figure 7). At 5 ft/s, greater reentrainment was seen with a baseline ash compared to a conditioned ash. However, at higher velocities, a greater level of reentrainment was seen with the conditioned ash. This result was surprising because the particle-to-particle binding forces are greater for the conditioned ash, which would be expected to result in less reentrainment. The reasons for this difference may be related to the cake structure. The conditioned ash forms a much more porous structure and may have a rougher surface structure. The baseline ash, on the other hand, tends to pack easily, resulting in a smoother surface that is less susceptible to reentrainment at higher velocities. To remove this possible bias, the procedure was changed so that the final layer of ash was sifted through a sieve onto the surface and was not smoothed with a knife edge. With this procedure, the surface structure for both the conditioned and baseline ashes should have been similar.

After changing the procedure, baseline and conditioning tests were conducted with both Monticello and Big Brown fly ashes. Results from the individual tests are shown in Figures 8 through 11. At each velocity, four repeat tests were conducted to establish the variability of the data. Results in Figures 8 through 11 are presented with error bars that signify plus or minus one standard deviation in the data. The measured levels of reentrainment appeared to be well behaved and highly repeatable. In most cases, the reentrainment was very low at 5 ft/s, but increased by 3 to 4 orders of magnitude at 25 ft/s. The highest velocity before catastrophic reentrainment occurred (when large chunks of ash would break loose and the ash layer would quickly erode away) was 25 ft/s for the Monticello ash and 35 ft/s for the Big Brown ash. This indicates that the Big Brown ash is more cohesive than the Monticello ash, and is consistent with the higher

HORIZONTAL REENTRAINMENT TEST SYSTEM



12

Figure 6. Horizontal reentrainment test system.

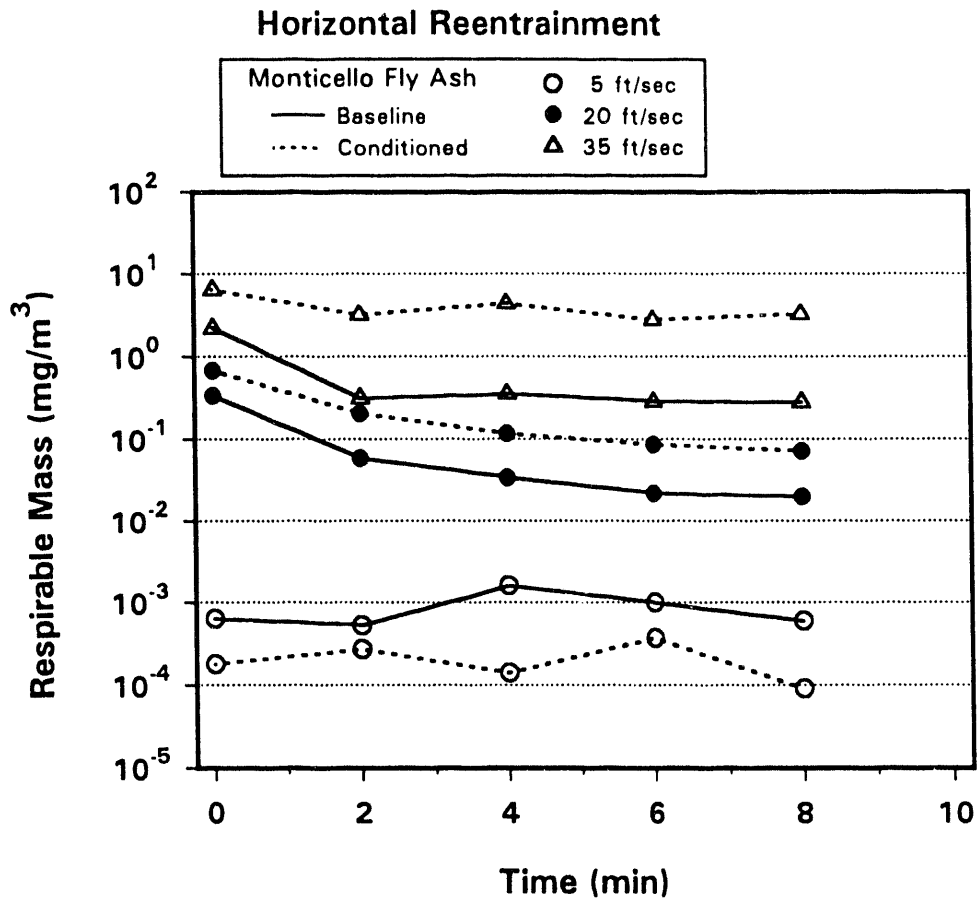


Figure 7. Reentrainment results with ash layer smoothed over with a knife edge.

measured tensile strength of the Big Brown ash. A comparison of the reentrainment for the baseline and conditioned ashes for the Monticello tests is shown in Figure 12, and the comparison for the Big Brown tests is shown in Figure 13. For all cases, except the lowest velocity, the reentrainment is lower for the conditioned samples, which is expected if the particle-to-particle binding forces are increased with conditioning. For the lowest velocity of 5 ft/s, the data indicate slightly higher reentrainment for the conditioned samples, but the values are just above background levels and appear to be within the variability of the data, so no difference should be inferred.

A second configuration was tested in which the gate was placed over the middle of the ash tray (rather than at the start of the ash tray) to see if the gate location would significantly affect the level of reentrainment. Results of these tests, shown in Figures 14 and 15, indicate the same effects of velocity and conditioning on reentrainment, thus the gate configuration does not appear to bias the results. With both gate configurations, the effect of conditioning on reentrainment was more pronounced with the Big Brown ash, which, as stated earlier, is consistent with the tensile strength data.

One of the objectives for conducting the horizontal reentrainment tests was to determine the velocity at which reentrainment occurs, relating the reentrainment velocity to cohesive measurements and, ultimately, to the particle-to-particle binding forces. An approximate calculation of the

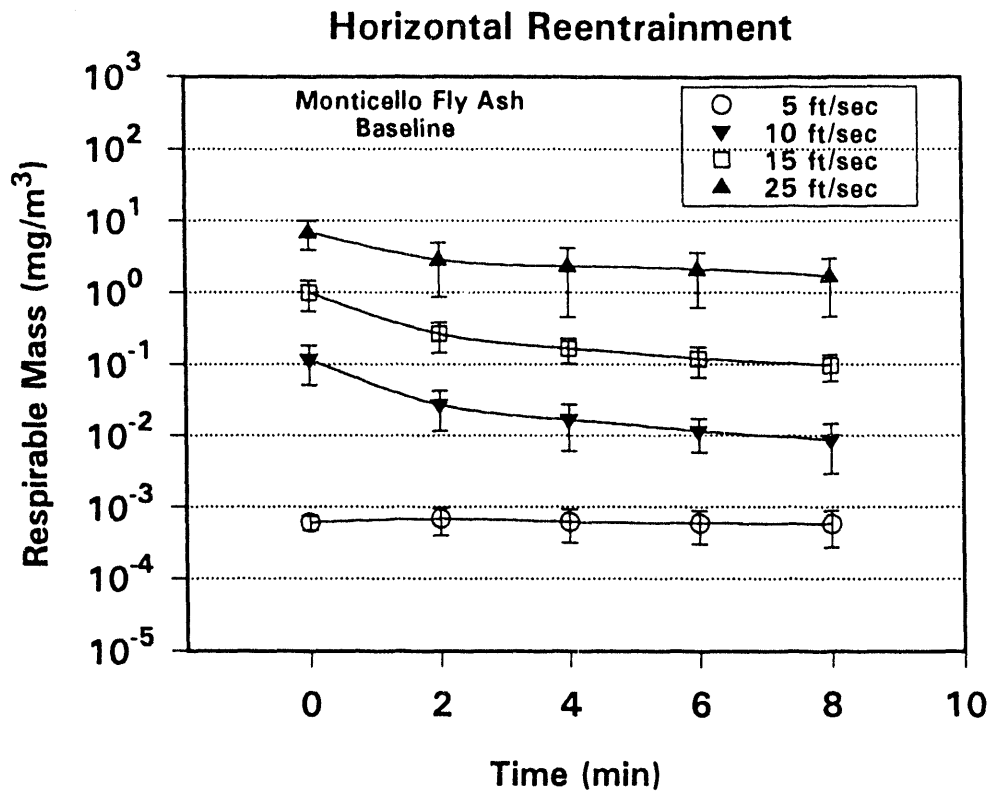


Figure 8. Reentrainment results for baseline Monticello fly ash with flow gate in front of ash layer.

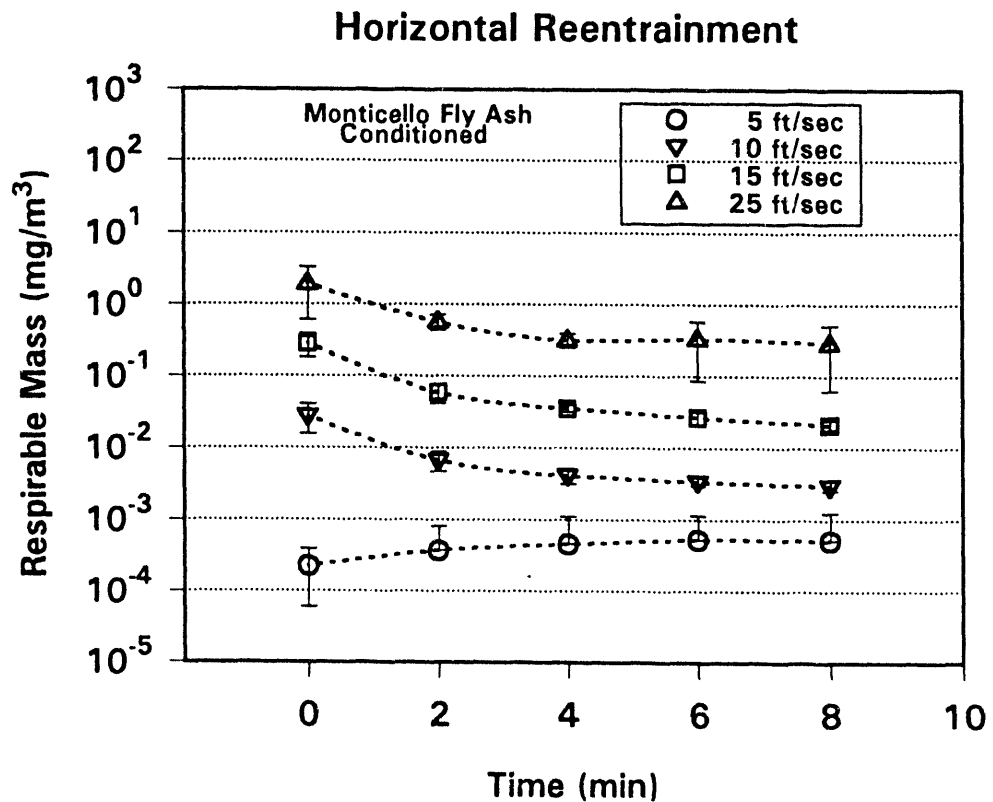


Figure 9. Reentrainment results for conditioned Monticello fly ash with flow gate in front of ash layer.

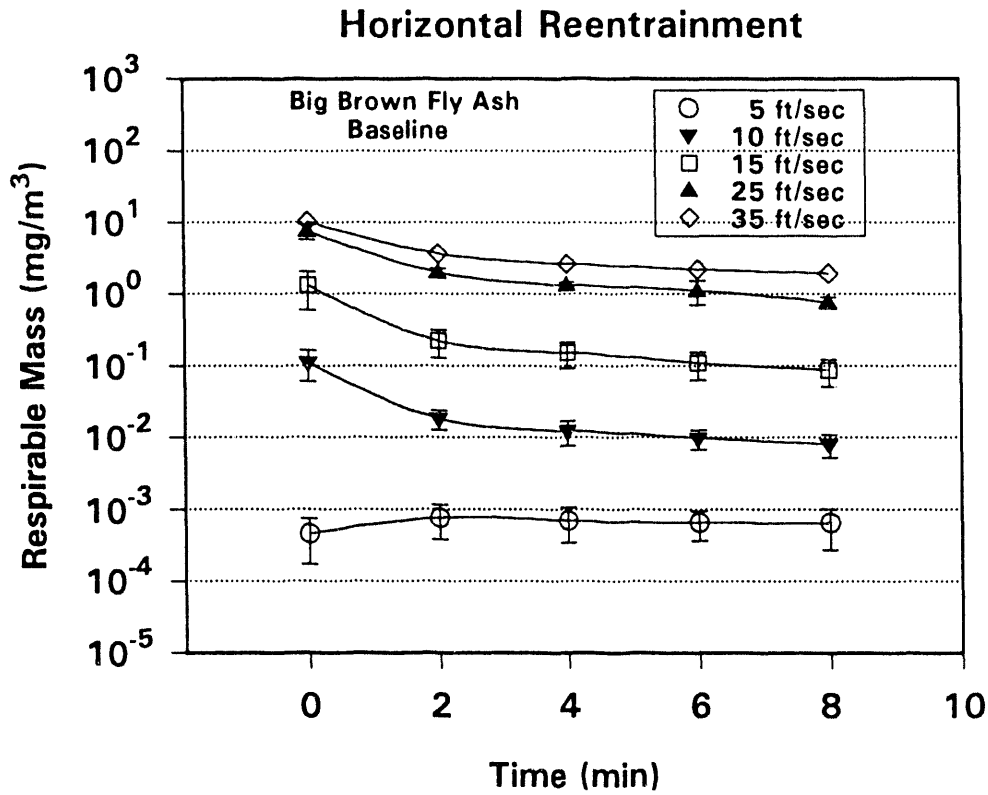


Figure 10. Reentrainment results for baseline Big Brown fly ash with flow gate in front of ash layer.

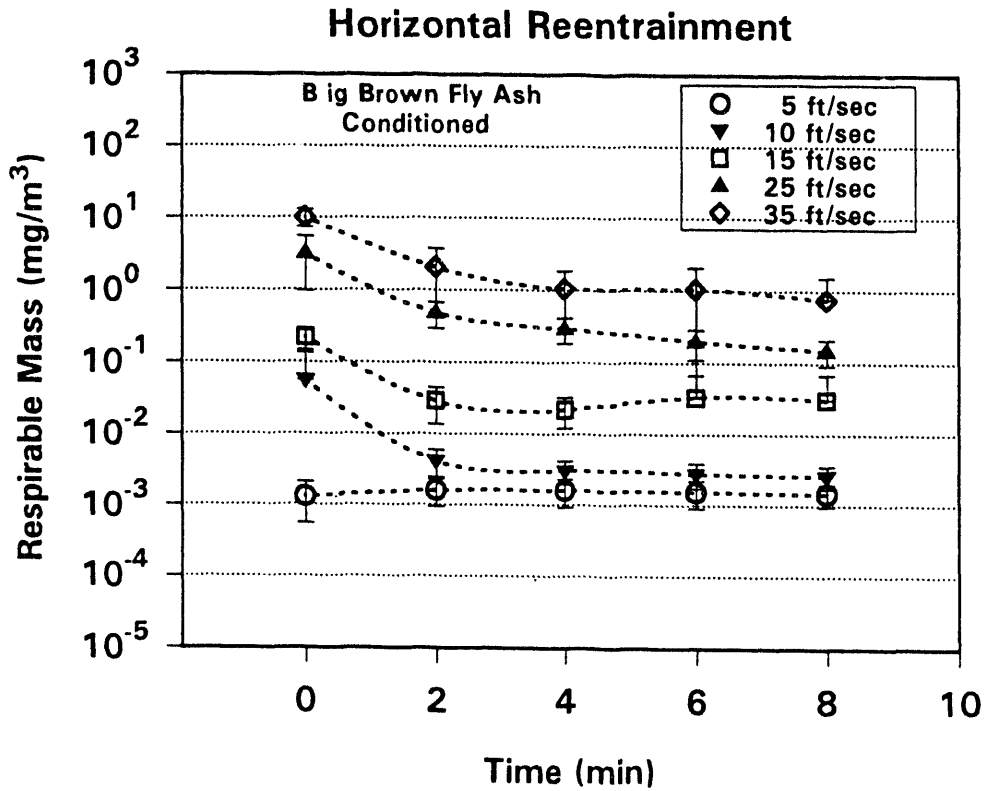


Figure 11. Reentrainment results for conditioned Big Brown fly ash with flow gate in front of ash layer.

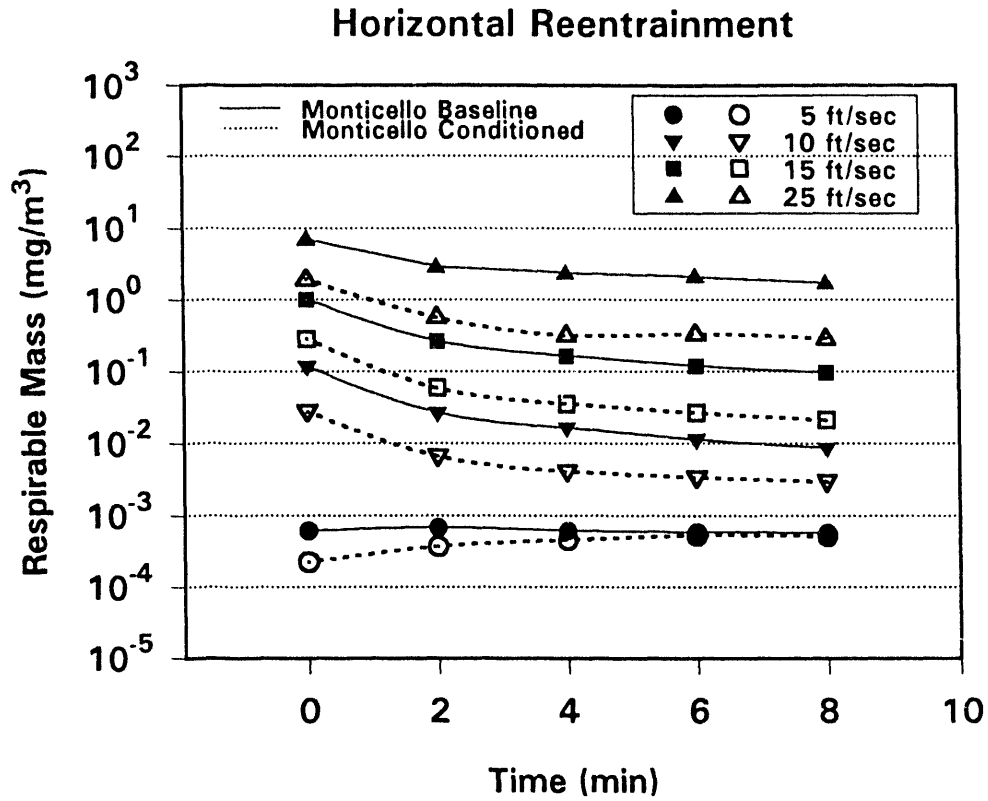


Figure 12. Comparison of reentrainment between baseline and conditioned Monticello fly ash with flow gate in front of ash layer.

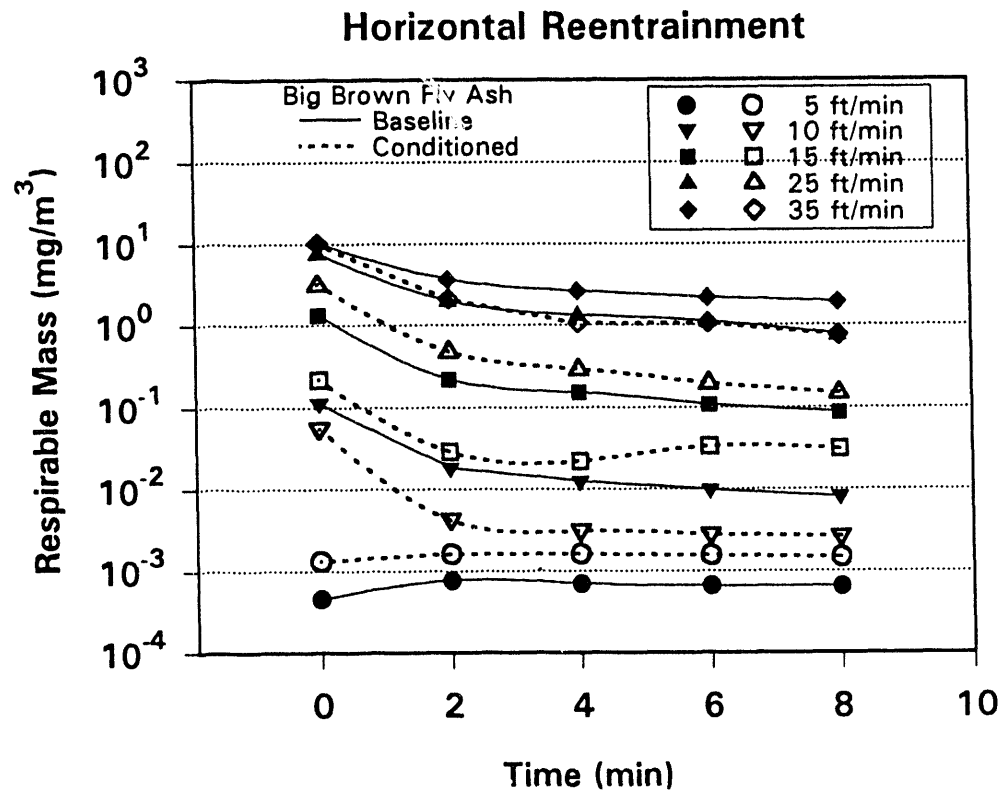


Figure 13. Comparison of reentrainment between baseline and conditioned Big Brown fly ash with flow gate in front of ash layer.

particle-to-particle binding forces can be made as follows: Measured tensile strengths for baseline and conditioned fly ashes with a mass median diameter (MMD) of about 13 μm have ranged from about 0.1 to 20 g/cm^2 . Assuming monosized 13- μm spherical particles and simple cubic packing (corresponding to a porosity of 47.6%), there would be 590,000 particles in contact in one cm^2 of area. This corresponds to a particle-to-particle binding force of 1.7×10^{-6} g, or 1.67×10^{-8} N for a dust tensile strength of 1 g/cm^2 . The actual particle-to-particle binding force is likely to be somewhat higher because porosity is typically greater than 47.6% and the pore structure will not result in a perfect packing arrangement. To reentrain a particle requires that the particle-to-particle binding forces must be overcome by a fluid drag force. For a 13- μm spherical particle, applying Stokes' law, the velocity at which the drag force is equivalent to a 1.67×10^{-8} N particle-to-particle binding force is 25 ft/s. This velocity is within the range of velocities for which significant reentrainment was noted. The actual conditions at the boundary layer, where the reentrainment occurred, are not known, but the Reynolds numbers for flow through the gate were well within the turbulent flow region. The most significant reentrainment tended to occur somewhat downstream from the gate and may have been influenced by turbulent eddies. Even though a laminar sublayer may exist at the dust surface, calculation of

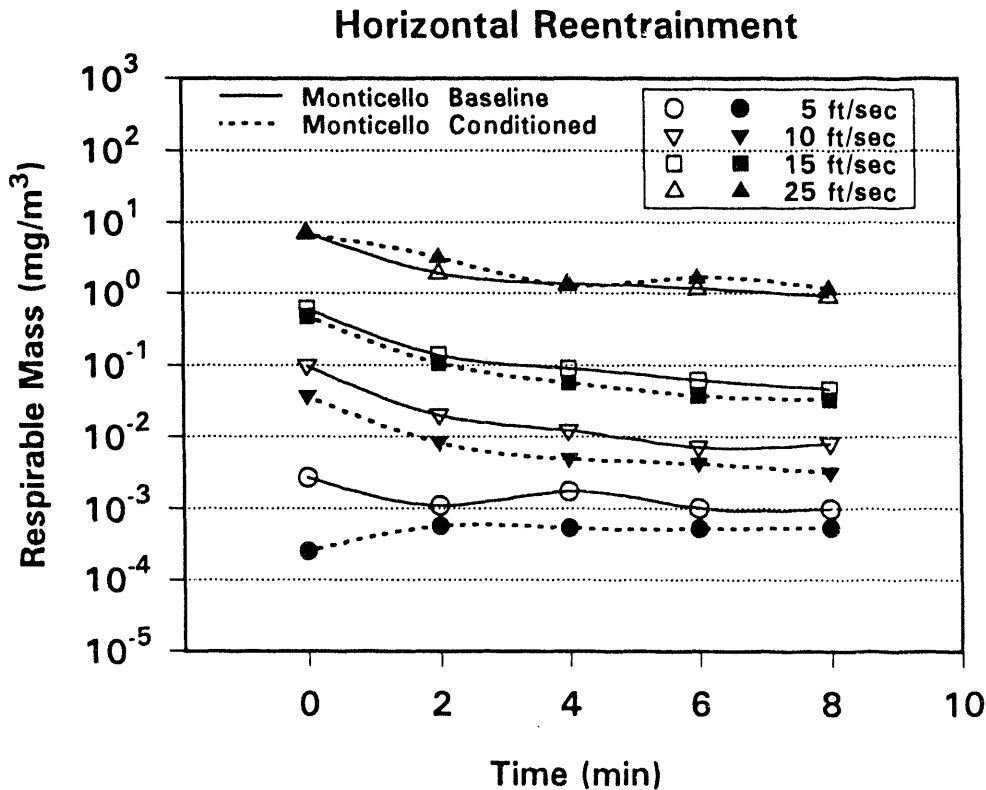


Figure 14. Comparison of reentrainment between baseline and conditioned Monticello fly ash with flow gate over the middle of ash layer.

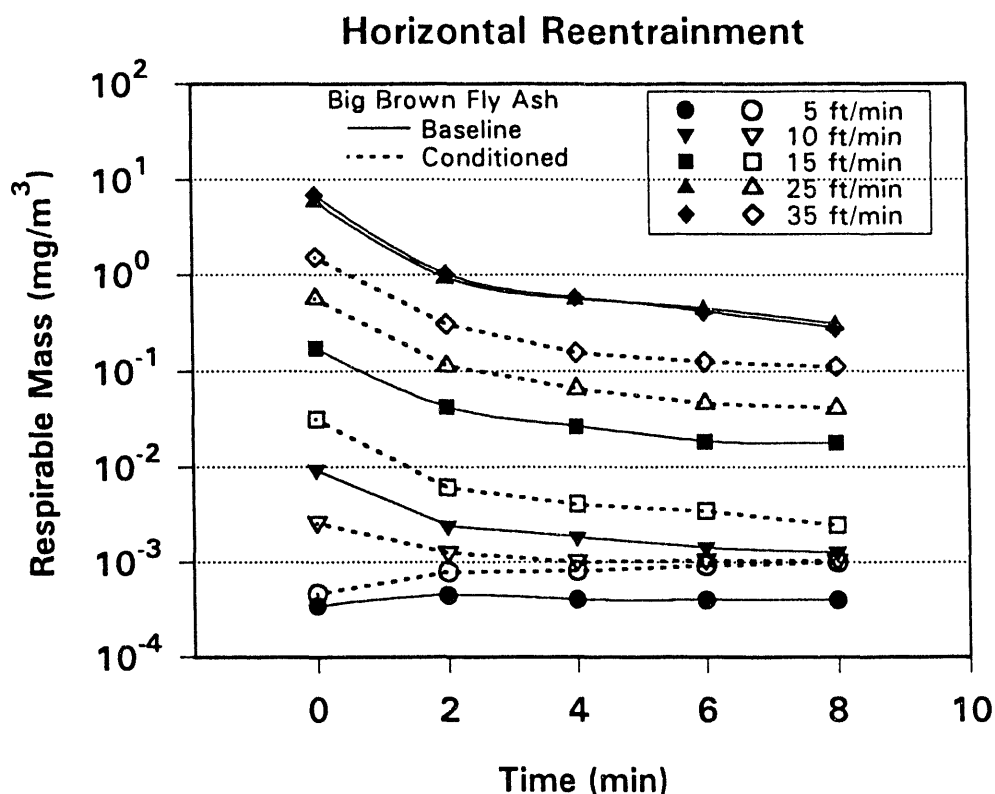


Figure 15. Comparison of reentrainment between baseline and conditioned Big Brown fly ash with flow gate over the middle of ash layer.

the exact drag force on the particles that were reentrained would be difficult because the exact location where the particles were initially at rest (in relation to the gate orientation) was not known, and turbulent conditions were present. Nevertheless, results indicate that fairly high velocities would be required to produce a Stokes' drag velocity of 25 ft/s to overcome a 1.67×10^{-6} N particle-to-particle binding force.

Note that velocities in the range from 5 to 25 ft/s are from 75 to 375 times greater than the common filtration face velocity of 4 ft/min used with pulse-jet baghouses. With a dust cake porosity of 50%, the actual velocity of the gas through the cake would be twice as great, but this is still 37 times smaller than the minimum velocity at which reentrainment was noted. This implies that particle reentrainment due to viscous drag within the bulk of a dust cake should not occur under normal filtration conditions because the velocities are too low. On the other hand, if velocities are greater than 5 ft/s, particle reentrainment is expected. One situation where local velocity can greatly exceed 5 ft/s is when pinholes develop. According to capillary flow calculations, the velocity through a 100- μ m diameter pinhole can be from 100 to 1000 times greater than the face velocity, or from 400 to 4000 ft/min (6.7 to 67 ft/s) for a typical face velocity of 4 ft/min (10). Therefore, once pinholes form beyond a critical diameter, it is difficult to bridge them again because of the potential for reentrainment along the edges. After bag cleaning, many of the larger pores are opened which can also result in localized high velocities. These pores must be quickly bridged again to

result in a high particulate-removal efficiency. Therefore, dusts with superior pore-bridging ability will obviously be collected with a better efficiency, and, if pore-bridging ability (or resistance to reentrainment) can be predicted from cohesive measurements, collection efficiency is also predicted from these measurements.

4.1.4 Conclusions from the Fine-Particulate Control Work

Ammonia and SO₃ conditioning can greatly improve the particulate collection efficiency and reduce the pressure drop of a fabric filter. While conditioning has been proven to be effective for a variety of coals, fabrics, and bag-cleaning methods, the basis for the amount of conditioning agents to be used is not well known. Tensile strength, porosity, pore-bridging ability, and reentrainment potential of baseline and conditioned fly ashes were measured to determine if they can be used as predictors of fabric filter performance. Although both tensile strength and porosity measurements correlate with pore-bridging ability and K₂, for fly ashes of similar particle sizes, tensile strength correlates more strongly with the pore-bridging ability of the dust, and measured porosity correlates more strongly with the K₂ of the dust. This implies that, for the best prediction of filter performance, both measurements should be conducted. However, more work is needed to quantify the correlations and to generalize them for other dusts.

4.2 **Impact of Coal Combustion on Atmospheric Visibility**

To evaluate the impact of fine-particulate emissions from coal-fired combustion systems on atmospheric visibility, a literature review was conducted. In order to achieve this goal, the literature survey has been organized to answer the following questions:

1. What are the causes of visibility impairment in the atmosphere? (For example, what sizes and concentrations of fine particulates in the atmosphere will result in significant visibility impairment?)
2. What is the composition of the visibility-reducing, fine-particulate aerosol, and what are the major sources of these fine particles?
3. What is the contribution from coal combustion to visibility-reducing fine particles in the atmosphere?
4. How are pollutants removed from the atmosphere, and what is the role of atmospheric chemistry in the production of secondary aerosols?
5. How would reduction of SO₂, NO_x, and fine-particulate emissions affect visibility?

4.2.1 Causes of Visibility Impairment

Reduction in visibility is the most immediately perceived effect of air pollution on the properties of the atmosphere; however, visibility is not easily defined by a single, directly measured parameter. Visibility monitoring indexes are usually divided into three groups: aerosol, optical, and scenic. Aerosol indexes include the particle-size distribution, composition, physical characteristics, and mass concentration of the atmospheric aerosol through which light passes. Optical indexes include

determination of the scattering, absorption, and extinction coefficients which characterize the ability of the atmosphere to alter the light passing through it. Scenic indexes include determination of visual range, contrast measurements, and documentation of the scene by photography. The visibility issue also includes human perception of scenic beauty and visual range and attempts to place a monetary value on the aesthetics of a scenic feature.

The transmittance of light through the atmosphere is attenuated by absorption and scattering by particles and gases. The extinction coefficient, b_{ext} , measures the total fraction of light that is attenuated per unit distance and is given by Equation 1:

$$b_{ext} = b_{sg} + b_{sp} + b_{ag} + b_{ap} \quad [Eq. 1]$$

where b_{sg} and b_{sp} are the light scattering coefficients of gases and particles, and b_{ag} and b_{ap} are the light absorption coefficients due to gases and particles. The extinction coefficient is usually expressed in units of reciprocal length.

Light scattering by gases (Rayleigh or natural blue-sky scatter by air molecules) is typically on the order of 10 to 12 Mm^{-1} . Rayleigh scattering decreases with altitude and is proportional to the air density. At sea level, Rayleigh scatter is approximately 13.2 Mm^{-1} at 0.52- μm wavelength, limiting visibility to about 296 km (184 miles). Nitrogen dioxide (NO_2) is the only gas present in significant quantities in the atmosphere that strongly absorbs light. It preferentially absorbs blue light, giving plumes a red, yellow, or brown color; however, the contribution of NO_2 to total extinction is usually minor. In a study of the brown haze which frequently plagues Denver, Colorado, NO_2 accounted for only 6% of the total extinction (17). Light scattering by particles is usually the largest component of extinction, except under extremely clean conditions when Rayleigh scatter predominates. Light scattering is primarily a function of the fine particles in the 0.1- to 2.0- μm size range, especially those with sizes comparable to the wavelength of visible light (0.4 to 0.7 μm). These particles are more effective at scattering light per unit mass than larger particles. Light absorption, on the other hand, is dominated by particles of elemental carbon (in the form of soot). Watson and others found large differences among elemental carbon contents of exhausts from motor vehicles powered by unleaded, leaded, and diesel fuels (18). As expected, diesel-powered vehicles were a major source of soot; however, large proportions of elemental carbon also came from unleaded gas-powered vehicles operating under very cold conditions.

Light-scattering efficiency is also affected by the absorption of water at high relative humidities. The six major components of fine-particulate aerosol are sulfates (typically associated with ammonium and/or hydrogen cations), organics, elemental carbon, ammonium nitrate, soil dust, and water (19). Sulfates and organics are the major contributors to fine-particulate mass. Fine sulfates typically account for over half of the fine-particulate mass in the East and less than half in the West (19). Nitrate contributions to fine mass are significant only in the West. Usually over 90% of both sulfates and nitrates are present as fine mass.

Results from the California Aerosol Characterization Experiment (ACHEX) showed that the major contributors to the light-scattering coefficient in the South Coast Air Basin of California were sulfates, nitrates, and organics

(20). An investigation of the relationship between visibility and aerosols in California showed that Rayleigh scattering accounted for only about 5% of the total extinction in most areas (21). Absorption by NO_2 accounted for 7% to 11% of the total extinction throughout the state, with sulfates responsible for 40% to 70% of the total extinction in Los Angeles and San Diego and 15% to 35% in the remainder of the state. In addition, nitrates accounted for 10% to 40% of the extinction in northern California. Black (graphitic) carbon, a significant contributor to visibility reduction, was not specifically accounted for in this study. However, a study by Conklin and others estimated that absorption by black (graphitic) carbon was responsible for as much as 17% of the total extinction in downtown Los Angeles in the wintertime (22). The contributions of fine-particulate species to the extinction coefficient from the Denver Brown Cloud Study are given in Table 1 (17). As shown in the table, elemental carbon was responsible for nearly 40% of the total extinction in Denver in the winter.

The contribution of a compound to extinction is not necessarily proportional to its contribution to fine mass. It may contribute more or less than its mass concentration to visibility impairment depending primarily on its size distribution and refractive index. For example, soot is approximately three times more efficient than SO_4^{2-} , NO_3^- , or organics in terms of visibility reduction per unit mass (23).

Fluctuations in relative humidity can have a significant impact on light extinction by aerosols. Water affects visibility only when it is in the liquid or solid phase. However, it is difficult to directly measure the contribution of liquid water to fine-particulate mass because of its rapid phase change. Typically, less than 0.01% of all water in a given volume exists in the liquid phase (except in fogs). Relative humidities above 70% greatly reduce visibility by increased light scattering due to the growth in size of hygroscopic aerosol species such as ammonium sulfate and sea salt.

Covert and others collected data on the humidity dependence of light scattering for different aerosol types (24). They classified the aerosols by their general chemical nature into four groups: marine, sulfate, urban/photochemical smog, and background continental (clean air from the dry southwest desert or high plains areas). The humidity dependence of the light-scattering coefficient can be expressed as the ratio $b_{sp}(\text{RH})/b_{sp}(\text{RH} = 30\%)$. At 60% relative humidity, acid sulfate, marine, and urban or photochemical aerosols had a mean ratio of 1.1 to 1.2, while sulfate salts and continental background aerosols had a ratio of 1.05 to 1.1. At 80% relative humidity, the scattering increased by a factor of 1.6 to 1.9 for all aerosol types, except continental background, which had a ratio of 1.3 or less.

Visual range is the maximum distance at which a large black object can be seen against the horizon sky in the daytime. Airport visual range determinations by human observers are the largest source of visual range data. In practice, an observer records whether or not a set of targets at known distances can be seen. Because nonideal (nonblack) and/or poorly placed targets are sometimes used, care must be exercised when comparing human observations of visual range with instrumental measurements of visibility. Visual range data derived using nonblack targets must be corrected for nonzero intrinsic target brightness to obtain standard visual range. Human

TABLE 1

Fine-Particulate Contribution to the Extinction Coefficient
for the Denver Wintertime Aerosol

Fine-Particulate Species	Mean Percent Contribution to b_{ext}
$(NH_4)_2SO_4$	20.2
NH_4NO_3	17.2
Organic Carbon	12.5
Elemental Carbon Total (scattering, 6.5; absorption 31.2)	37.7
Other	6.6
NO_2	<u>5.7</u>
Total	100.0

observations of visual range at airports are scheduled to be replaced by forward-scattering monitors in the mid-1990s (25).

The relationship between visual range and extinction is given by the Koschmeider equation (Eq. 2), where x is the visual range and b_{ext} is the extinction coefficient.

$$x = \frac{3.912}{b_{ext}} \quad [\text{Eq. 2}]$$

The constant in the equation is based on a contrast threshold of 0.02. The contrast threshold is the smallest increment of contrast that can be detected by the human eye and varies from observer to observer. Values of 0.0077 to 0.06 have been reported for the contrast threshold, corresponding to a range of 2.8 to 4.9 for the value of the constant in the Koschmeider equation. Typically, a value of 0.02 is used for visual range calculations. The Koschmeider equation ignores the earth's curvature and assumes that the atmosphere is homogeneous. The equation also assumes a perfectly black target observed against an ideal white background. The equation is of limited usefulness under partly cloudy skies because it assumes equal illumination of all parts of the atmosphere in the horizontal plane.

4.2.2 Source Contribution to Visibility Impairment

Evidence exists for a background level of atmospheric aerosol based on ambient aerosol measurements in remote areas (especially in the southern hemisphere). Measurements of light scattering at Point Barrow, Alaska, and Mount Olympus, Washington, using an integrating nephelometer, agree in magnitude, and are also in agreement with other measurements of light-

scattering and turbidity made in remote locations (26). Values of the background aerosol levels estimated from measurements at remote locations, compilations of man-made and natural sources, and regression studies using tracers are presented in Table 2 for the eastern and western United States. Rayleigh scatter (46%), organics (22%), and water (19%) are the major contributors to natural extinction in the East. In the West, the major contributors to natural extinction are Rayleigh scatter (64%), soil dust (including coarse particles) (14%), and organics (11%) (19).

The best visibility occurs in the mountainous Southwest with a median visibility of greater than 110 km (70 miles). Annual median visibilities are less than 24 km (15 miles) east of the Mississippi and south of the Great Lakes. The difference in median visibility is partially caused by the higher ambient relative humidities, greater vegetation densities (conducive to the formation of secondary aerosols), and hygroscopic marine aerosols in the East (27). In a study of visibility observations of three distinct mountains at Blue Hill, Massachusetts, from 1889 to 1958, researchers attempted to determine whether visibility was ever as good in the East as it is presently in the Southwest (28). Although two peaks in haziness corresponded roughly with two peaks in combined coal and wood burning (1910-1920 and 1940-1950), they were unable to state conclusively that fossil fuel burning was responsible for the increased haziness because of the variability in the data.

A study of haze in Shenandoah National Park concluded that 78% to 86% of the extinction coefficient was of anthropogenic origin. Of the 14% to 22% from natural causes, sulfates and associated water contributed 3% to 11% to the extinction coefficient; organics, 5%; Rayleigh scattering, 5%; and crustal dust, 1% (29). The sulfate estimate was based on measurements in remote areas; however, the estimate of 11% (based on measurements in remote South Dakota) may be more of a background value than the contribution from natural sources due to the general sulfate contamination of the northern hemisphere. The estimate of 3% (from measurements in South America) may be more reasonable. All elemental carbon was assumed to be anthropogenic in origin, and a ratio of 1.5 to 1 was used for the anthropogenic organic/elemental carbon emission ratio in the estimate of the natural source contribution of organics. Due to uncertainties

TABLE 2
Natural Background Levels of Atmospheric Aerosols

	Average Concentration		Error Factor
	East ($\mu\text{g}/\text{m}^3$)	West ($\mu\text{g}/\text{m}^3$)	
Fine Particles (<2.5 μm)			
Sulfates as NH_4HSO_4	0.2	0.1	2
Organics	1.5	0.5	2
Elemental Carbon	0.02	0.02	2-3
Ammonium Nitrate	0.1	0.1	2
Soil Dust	0.5	0.5	1.5-2
Water	1.0	0.25	2
Coarse Particles (2.5-10 μm)	3.0	3.0	1.5-2

in carbon speciation and in the organic/elemental carbon ratio, the natural organic contribution could be as large as 10% if all measured carbon were organic and from natural sources. Using values of 3% and 10% for the sulfate and organic contributions, respectively, and a more reasonable value of 3% for Rayleigh scattering, results in a natural source contribution to the extinction coefficient of 12% to 17%.

As part of the 1987-1988 Denver Brown Cloud Study (30), coal-fired power plants in Denver were switched to natural gas at about 2-week intervals. Previous studies had implicated sulfates as a significant contributor to the Brown Cloud. It was anticipated that a 70% reduction in SO_2 as a result of fuel switching would result in a significant reduction in sulfates. However, the anticipated reduction in sulfates did not materialize. Sulfate showed no change between coal- and gas-burning periods despite a two fold reduction in SO_2 emissions. Long-range transport of air pollutants from the Pawnee power plant in northeast Colorado was identified as a source of secondary particulates, complicating observations in Denver, especially when average concentrations were considered. Therefore, researchers have suggested that the entire South Platte River basin and its complex meteorology must be considered as a source region for Denver air pollution.

After eliminating periods of potential transport from the Pawnee power plant, the data indicated a distinct reduction in sulfates during gas-burning periods (30). However, the change was small compared to other pollutant species concentrations, including nitrates and elemental and organic carbon. Sufficient data that were unaffected by transport from the Pawnee power plant were not available to identify the effect of individual sulfate sources. Moreover, during a number of severe pollution episodes, neither transport from Pawnee nor other coal-fired power plants could be identified as major contributors. Further understanding of the role of ground-based sources of precursors to the formation of the Brown Cloud await the availability of a complete chemical data set from the study.

A strike in 1967-1968 which closed copper smelters in the Southwest for 9 months provided an opportunity to study the relationship between smelter emissions and ambient sulfate concentrations. At the time of the strike, copper production accounted for over 90% of the SO_x emissions and less than 1% of the NO_x emissions and, therefore, affected visibility primarily through its contribution to sulfate loadings. During the strike, substantial decreases in sulfate occurred at Tucson, Phoenix, Maricopa County, White Pine, and Salt Lake City, all within 113 km (70 miles) of copper smelters. Sulfates also dropped by about 60% at the Grand Canyon and Mesa Verde National Parks, 325 to 500 km (200 to 300 miles) from the main smelter area in southeast Arizona. Phoenix experienced a large decrease in sulfate concentration which was accompanied by a substantial improvement in visibility.

A strike in July 1980 shut down 9 of 11 copper smelters in Arizona and New Mexico for three months. After studying sulfate emissions and ambient air levels before, during, and after the strike, researchers concluded that the largest sulfate concentrations at remote sites in Arizona and southern Utah from August 1979 to July 1980 were accompanied by wind trajectories from copper smelters. During the strike, mean sulfate concentrations throughout Arizona decreased 50% to 90% from the previous summer.

The Winter Haze Intensive Tracer Experiment (WHITEX) was designed to evaluate the feasibility of using various receptor modeling techniques to attribute emissions from a single point source, the Navajo Generating Station (NGS), to the visibility impairment in a number of national park areas, including the Grand Canyon (31). The NGS is a 2250-MW coal-fired utility plant located at Page, Arizona. Tracer mass balance regression (TMBR) analysis of data from the Hopi Point, Grand Canyon, monitoring site was used to estimate the contribution of the NGS to secondary sulfates and nitrates at the Grand Canyon. A tracer, deuterated methane (CD_4), was released from one of the three stacks at the NGS during the study. CD_4 is nonreactive and stable (even at elevated temperatures) with a presumed deposition velocity close to zero. It is not emitted by other sources and has a background concentration of 1 part in 10^{16} . Attempts to vary the tracer emission rate in proportion to the plant load were not very successful; therefore, the data were "standardized" to a constant CD_4 emission rate for analysis. Results from the study indicated that the NGS contributed from 70%-80% of the sulfate concentration at the Grand Canyon, with copper smelters contributing 10%-30% (30). Background sulfate concentration was estimated between 0% and 10%. Results from the Differential Mass Balance (DMB) Model, also used in the WHITEX study, found that NGS contributed 71% of the ambient sulfate measured at Hopi Point (32).

Based largely on the results of this study, the EPA has ruled that NGS must phase in scrubbers between 1997 and 1999, reducing the plant's SO_2 emissions 90% (33). This ruling marks the first, and perhaps only, time the EPA has acted solely to protect visibility in a national park.

4.2.3 Atmospheric Chemistry

The gas-phase conversion of SO_2 and NO_x to H_2SO_4 and HNO_3 is controlled by the concentration of the OH^- radical. The estimated residence time of SO_2 in the atmosphere has been reported to range from 4 to 40 days (34). The gas-phase conversion rate of SO_2 by the OH^-SO_2 reaction varies from 0.7%/hr in the summer to 0.12%/hr under winter conditions. Assuming the same OH^- levels, conversion of NO_x to HNO_3 was estimated to vary from 6.2%/hr in the summer to 1.1%/hr in the winter (33). Sulfuric acid formed in the gas-phase immediately associates with water molecules to form sulfuric acid aerosol. Nitric acid remains as a vapor until it is absorbed by a cloud or raindrop or reacts with ammonia to form ammonium nitrate. Ammonium nitrate is present as particles only when equilibrium is achieved with ammonia and nitric acid gases in the environment. Conversion of SO_3 to sulfuric acid aerosol in the gas-phase depends primarily on the concentration of the OH^- radical. The concentration of the OH^- radical depends indirectly on the NO_x and hydrocarbon levels, as well as on sunlight intensity. The conversion of SO_2 by the OH^- radical is linear; however, it is influenced in a complex (most probably nonlinear) manner by the concentrations of NO_x and hydrocarbons and their effect on the OH^- concentration.

Additional sulfate is formed by the absorption of SO_2 by droplets of water, followed by aqueous-phase oxidation. The amount of SO_2 absorbed depends on the SO_2 concentration and on the pH of the solution. Hydrogen peroxide (H_2O_2) is a major aqueous-phase oxidant; however, its concentration in the atmosphere is typically only in the parts per billion (ppb) range. Therefore, in this case, the oxidation of SO_2 to sulfate may be limited by the concentration of H_2O_2 . Ozone (O_3) is also an effective oxidant; however, its

oxidation potential decreases rapidly as the pH decreases, suggesting that H_2O_2 may be a more effective oxidant. At the moderately acidic conditions normally found in atmospheric water droplets, dissolved SO_2 ionizes to bisulfite. This ion is then oxidized to sulfate by any of several oxidizers. It is believed that in-cloud oxidation of S(IV) to sulfate is dominated by H_2O_2 , because oxidation by O_3 is suppressed, particularly at the low pH levels typically found in cloud water droplets. Buffering agents such as NH_3 and carbonates from soil dust can raise the pH sufficiently for the oxidation of SO_2 by O_3 to occur. Ammonium sulfate is formed primarily by the reaction of ammonia with sulfuric acid.

In laboratory experiments on the gas-solid reaction of SO_2 with carbon, Novakov and others found that graphite and soot particles oxidize SO_2 in air (35). Soot exposed to humidified air in the presence of SO_2 produced more sulfate than soot exposed to dry air. They also found a correlation between ambient concentrations of carbon and SO_4 in Los Angeles, which supports their hypothesis that carbon (soot) oxidation may be an important pathway for sulfate formation. The catalytic formation of sulfate on soot particles may be of greatest significance in the open atmosphere, particularly near combustion sources where the concentrations of SO_2 and soot are both high.

Secondary particles formed from alkenes having seven or more carbon atoms (cyclic olefins, diolefins, and terpenes) produce considerable visibility impairment. For example, secondary organics produced from cyclic olefins and diolefins generally are in the 0.1- to 0.3- μm size range. Particle formation consists of supersaturation of the gas-phase and subsequent condensation on pre-existing particles. In Los Angeles, the average conversion of precursor organic vapors to organic particles was estimated to be 1% to 2%/hr.

Pollutants are removed from the atmosphere by dry and wet deposition. In dry deposition, the pollutant is absorbed at the surface of the earth by soil, water, or vegetation. Dry deposition is controlled by a number of processes, including turbulent mixing of the atmosphere and the chemical and biological interaction of the pollutant and the surface on which it is deposited. Wet deposition refers to absorption of the pollutant into water droplets and subsequent removal by precipitation. Wet deposition, therefore, is governed by cloud physics and gas- and liquid-phase chemistry. Dry deposition is characterized by the deposition velocity, v_d , which is defined as the ratio of the flux of the material to the earth's surface and the ambient atmospheric concentration of the species. The highest deposition velocities generally occur during the day when atmospheric mixing is the greatest and the leaf stomata of vegetation are open. Deposition velocities range from 0.1 to 2.3 cm/s for SO_2 , with a median value of 0.7 cm/s (32). Typical deposition velocities for fine particles range from 0 to 1.0 cm/s, with a median value of 0.2 cm/s. The dry deposition process for gases is influenced by many factors, including seasonal effects, diurnal effects (sunlight, atmospheric stability), and meteorological effects (humidity, wind speed, temperature).

4.2.4 Coal Combustion and Visibility

As is shown by the following discussion, secondary sulfates from coal combustion contribute significantly more to visibility impairment than primary fly ash emissions. Two scenarios are evaluated with a coal assumed to have

the following characteristics: higher heating value of 12,000 Btu/lb, 1.5% sulfur and 8% ash.

Scenario #1:

The facility has an ESP with a collection efficiency of 95% for particulate matter (PM) with no SO₂ scrubbing. The resulting emissions would then be 2.5 lb SO₂/10⁶ Btu and 0.27 lb PM/10⁶ Btu. The mass ratio (SO₂/PM) would then be 9.3.

Scenario #2:

In this case New Source Performance Standards must be met, which for this coal would be 0.6 lb SO₂/10⁶ Btu and 0.03 lb PM/10⁶ Btu. The mass ratio (SO₂/PM) for this case would be 20:1.

Assuming the MMD of the PM emissions is 5 μm (D_p) and 0.3 μm (D_s) for secondary sulfates, and since the number of particles for a constant mass is directly related to the cube of the particle diameter, the particle number ratio (D_p³/D_s³) is 4630. For scenario #1 there would be approximately 43,000 (9.3 x 4630) more secondary sulfate particles than other emitted particles. For scenario #2, the same calculation shows that there would be 93,000 (20 x 4630) more secondary particles emitted. This clearly shows that secondary sulfate particles are of primary concern.

4.2.5 Effect of Reduced Emissions on Atmospheric Visibility

Improved visibility should be an important indirect result of the reduction in SO₂ and NO_x required by the Clean Air Act Amendments. However, controlling SO₂ and NO_x emissions are not necessarily the only way to reduce ambient sulfate and nitrate concentrations. In parts of the western United States where the contribution of fine ammonium nitrate to visibility reduction is significant, perhaps controlling ammonia from cattle feedlots would be appropriate for reducing ambient nitrate levels. The ammonium ion is found predominantly in the optical-scattering size range or below. It is likely secondary in origin, produced by the neutralization of acid sulfate particles by ambient NH₃. Reducing urban ozone levels by controlling hydrocarbon and/or nitrogen oxide emissions may slow oxidation of SO₂ to sulfate, reducing ambient sulfate concentrations. Due to the complex processes which control the formation of secondary sulfates and nitrates in the atmosphere, controlling emissions of SO₂ and NO_x may not yield proportionate reductions in ambient sulfate and nitrate concentrations and a corresponding improvement in visibility.

As discussed earlier, the aqueous-phase oxidation of SO₂ to sulfate may be oxidant-limited. Therefore, at distances from the source where the molar concentration of SO₂ is greater than the molar concentration of H₂O₂, the wet deposition rate is a constant that depends on the oxidant concentration. At greater distances from the source where the SO₂ concentration is less than the oxidant concentration, the wet deposition rate becomes proportional to the SO₂ concentration as the distance from the source increases. Therefore, if emissions are reduced, the change in wet deposition rate will not be proportional to the change in emissions except at great distances from the source. Where the SO₂ concentration is greater than the oxidant concentration, the reduction in emissions will have no effect on the deposition rate. The formation of nitric acid is dependent on the level of photochemical activity in the atmosphere. Therefore, nitrate concentrations

may not respond linearly to a change in NO_x emissions depending on how the changes affect the OH⁻ level.

The regional impacts on visibility and acid deposition (RIVAD) model, a plume-segment Lagrangian model designed to evaluate regional source-receptor relationships, was used to evaluate the effects on regional visibility of a 12-million ton per year reduction in SO₂ emissions in the 31 eastern states (36). The model calculated time-dependent air quality impacts by tracking the transport, dispersion, chemical conversion, and deposition of SO₂ and NO_x emissions in a plume segment representing 3-hour emissions. Three-hour time steps in upper-air wind fields, precipitation fields, atmospheric stability, and mixing heights were used to describe regional meteorology. Diurnal and seasonal variations in SO₂ oxidation rates were calculated in the model using a chemical module consisting of 8 reactions.

In 1980 total SO₂ emissions in the 31 eastern states were estimated at 21.9 million tons, with power plants accounting for 74%. The total SO₂ emission inventory for North America was estimated at 31.8 million tons, with United States sources contributing 83% of the total and the 31 eastern states contributing 69%. A 12-million ton reduction in SO₂ emissions would result in reductions of 55% and 38% in SO₂ emissions for the 31 eastern states and the United States overall, respectively. Based on simple mass balance calculations, one would expect a corresponding reduction in SO_x concentrations. The RIVAD model improves on these estimates by accounting for the locations of sources and the time- and space-dependent meteorological patterns that affect the transport, dispersion, transformation, and deposition of SO₂ emissions.

Calculations based on the RIVAD model showed that in 1980 sulfate accounted for 30% to 70% of the annual average light extinction in the eastern United States. Sulfates accounted for 70% of the extinction in the Appalachian Mountains of Pennsylvania, Maryland, West Virginia, and Virginia. Other researchers have shown that sulfates and associated water account for approximately 50%, on average, of the light extinction that causes haze, and up to 75% of the light extinction in nonurban areas in the summer.

Regional reductions in sulfate concentrations from a 12-million ton reduction in SO₂ emissions range from approximately 30% to a maximum of 54%. Reductions of more than 50% occur in Kentucky, West Virginia, Virginia, Tennessee, and North Carolina. Most highly populated areas in the Midwest and Northeast would experience a reduction in sulfate concentrations of 40%-50%. These predicted sulfate concentrations are based on the assumption that regional sulfate concentrations are linearly related to SO₂ emissions. However, recent work has suggested that sulfate may be related nonlinearly to regional SO₂ emissions changes partially because the in-cloud oxidation of SO₂ may be limited by the pH-dependence of SO₂ solubility.

Regional SO₂ emission controls would improve visibility by reducing the contribution of sulfates to light extinction and the total light extinction. The visual range was calculated using the following equation:

$$r_v = \frac{3}{b_o + b_s}$$

where b_o is the light extinction due to fine-particulate aerosols other than sulfate, and b_s is the sulfate light-scattering coefficient. The authors chose to use 3 rather than 3.912 as the constant in the equation because they concluded that it gave better agreement between airport observations of visual range and light extinction. A constant of 3 is obtained when a contrast threshold of 0.05 rather than 0.02 is used.

The sulfate light-scattering coefficient, b_s , depends on relative humidity and on whether the sulfate exists as H_2SO_4 , $(NH_4)HSO_4$, or $(NH_4)_2SO_4$, due to the variable mass of liquid water and associated cations:

$$b_s = K f(RH) [SO_4]$$

where K is the scattering efficiency per dry mass of sulfate anion, $f(RH)$ is a dimensionless factor that accounts for the associated liquid water, and $[SO_4]$ is the concentration of the SO_4 anion.

The value of K depends strongly on the particle-size distribution. In this analysis, K was calculated from Mie theory using a mass median diameter of $0.3 \mu m$ and a geometric standard deviation 2.0 (a typical sulfate aerosol size distribution) and the sulfate species density ($1.8 g/cm^3$). The form of sulfate affects the value of K because of the difference in cation mass associated with the sulfate anion; $K=4.6$, 4.0 , and $3.4 m^2/g$ for $(NH_4)_2SO_4$, $(NH_4)HSO_4$, and H_2SO_4 , respectively.

The value of $f(RH)$ depends strongly on the molecular form of sulfate and on the relative humidity. In nonurban areas of the eastern United States, sulfate typically exists as $(NH_4)HSO_4$, whereas in urban areas it exists as $(NH_4)_2SO_4$. The average and midday humidities in the East are 70% and 60%, respectively. The value of $f(RH)$ is 1.0 for $(NH_4)_2SO_4$, and 2.2 and 2.9 for $(NH_4)HSO_4$ at relative humidities of 60% and 70%, respectively. However, $(NH_4)_2SO_4$ can also have values in the range of 2.2 to 2.9 due to hysteresis. If $(NH_4)_2SO_4$ is cycled from a humidity above its deliquescence point (approximately 80% RH) due to diurnal changes during the day, or over a shorter time period as it is mixed from higher (colder) elevations, the aerosol exhibits hysteresis and does not reach its equilibrium water content but instead exists as a supersaturated droplet. Therefore, for a typical midday relative humidity of 60%, the lowest humidity (highest temperature) of a diurnal cycle, the overall light-scattering efficiency of ammonium sulfate could be significantly higher than the theoretical value of $4.6 m^2/g$.

Significant reductions in sulfate concentrations may tend to lower the light-scattering efficiency per unit mass as well as the sulfate mass. Therefore, a reduction in SO_2 emissions may have a greater than proportional effect on light extinction because of the simultaneous reduction in both the sulfate concentration and its light-scattering efficiency. If sulfate concentrations are reduced by a factor of 2 while ammonia concentrations remain constant, the regional average (nonurban) aerosol may change from $(NH_4)HSO_4$ to $(NH_4)_2SO_4$, decreasing the regional-average sulfate light-scattering efficiency from 8.8 to $4.6 m^2/g$. This decrease would occur only in nonurban areas since urban aerosol already exists as $(NH_4)_2SO_4$. However, if

hysteresis occurs, the reduction in scattering efficiency may not occur in urban areas either. Other factors, such as a shift in the sulfate aerosol size distribution, could also change the scattering efficiency of the atmosphere as regional SO₂ emissions are changed. Higher ambient NH₃ concentrations may result from a reduction in sulfate concentration, producing more nitrate aerosol from nitric acid vapor. The presence of a film of organics on the aerosol surface could affect the growth and scattering efficiency of the sulfate aerosol.

Due to uncertainties in the ammonium/sulfate ratio and the potential hysteresis effects associated with changing relative humidity, the authors considered the following three assumptions for the sulfate light-scattering efficiency in estimating regional visibility improvement:

1. Assume sulfate exists as (NH₄)₂SO₄ with a scattering efficiency of 4.6 m²/g (at 60% RH).
2. Assume sulfate exists as (NH₄)HSO₄ with a scattering efficiency of 8.8 m²/g (at 60% RH), or as (NH₄)₂SO₄ undergoing significant hysteresis associated with temperature and relative humidity cycling so that its liquid water content and scattering efficiency are higher than equilibrium values.
3. Assume sulfate exists initially as (NH₄)HSO₄ with a scattering efficiency of 8.8 m²/g (at 60% RH), and after SO₂ emissions controls, with sulfate effectively halved, as (NH₄)₂SO₄ with a scattering efficiency of 4.6 m²/g.

Empirical evidence for the effect of hysteresis on sulfate light scattering lead the authors to use the second assumption to estimate regional visibility improvements resulting from SO₂ emissions control.

Model calculations of the percentage improvement in visibility resulting from a 12-million ton reduction in annual SO₂ emissions are given for a 31-state region in the eastern United States, and for the Ohio River Valley, where the existing visibility is the lowest and the predicted change in sulfate concentration is the highest. The calculations were performed assuming both a linear and nonlinear relationship between SO₂ emissions and sulfate concentration. The nonlinear relationship used assumed that a 50% reduction in SO₂ emissions would result in only a 35% reduction in the sulfate concentration. The percentage improvement in average annual visibility for the 31-state region was 26% assuming a linear relationship between SO₂ emissions and sulfate concentration and 18% assuming a nonlinear relationship. For the Ohio River Valley, the improvement in visibility was 35% assuming a linear relationship and 25% assuming a nonlinear relationship. The model predicted a 50% increase in average annual visibility in the Appalachian Mountains, where sulfates account for up to two-thirds of the existing light extinction. The most significant uncertainties in this analysis concern the possible nonlinearity in the SO₂-sulfate relationship and the effect of hysteresis on the sulfate light-scattering efficiency.

4.2.6 Summary of Literature Review on Atmospheric Visibility

Visibility impairment in the atmosphere is primarily caused by light attenuation by fine particles (<2.5 μm). Secondary fine-particulate matter

formed in the atmosphere from SO₂ and NO_x precursors are a major source of these fine particles. Other major constituents of fine atmospheric particles are organics, elemental carbon, ammonium ion, soil dust, and water vapor. Water vapor contributes to visibility impairment primarily when the relative humidity is high enough to cause growth in the size of hygroscopic aerosols such as ammonium sulfate. Since coal combustion is a major source of SO₂ (and, subsequently, atmospheric sulfates), some visibility impairment must be attributed to coal combustion. Visibility impairment in the Grand Canyon by secondary sulfates and nitrates from the Navajo Generating Station is a case where the visibility impairment was specifically attributed to a coal-fired power plant. In response, the EPA has required that scrubbers be installed at the Navajo plant to correct this visibility impairment. However, the exact contribution of coal combustion to regional haze is generally not known, and the benefits to be derived from much stricter emission controls on coal-fired power plants are difficult to assess. It appears logical that if SO₂ and NO_x emissions from coal-fired power plants were reduced by 50%, there would have to be an eventual reduction of 50% of the sulfates and nitrates in the atmosphere that originated from coal combustion. However, because of the variable contribution to visibility impairment from coal combustion that might occur in a given location, the overall effect on visual range for that location might be small.

Results from this literature review indicate there is a complex relationship between emissions from coal combustion sources and visibility impairment, but that coal combustion may be a significant contributor in some cases.

4.2.7 Summary of Selected Literature Sources

Begley, S. "The Benefits of Dirty Air - Pollution May Negate the Greenhouse Effect," *Newsweek* 1992, 1, 54.

Researchers from seven universities and federal agencies have reported that the same pollutants responsible for acid rain may ward off global warming. It has been generally known for some time that sulfate aerosols reflect sunshine and act as cloud condensation nuclei, which reflect solar radiation back into space and result in cooling of the Earth. However, according to the latest research, this cooling is just about equal to the heating effect due to "greenhouse gases" such as CO₂, and therefore likely offsets global warming to a large degree. Thus there has been less warming of the Earth than predicted by simple greenhouse models.

It has also been postulated that sulfates may defend the Earth against the disappearing ozone layer. A researcher at the National Oceanic and Atmospheric Administration (NOAA) has suggested that scattering of ultraviolet (UV) radiation by fine sulfate is the reason why, despite a 5% decrease in wintertime ozone in the northern hemisphere over the last decade, there is not much more UV radiation reaching the ground.

Burns, S.; Frey, S.J.; Chow, J.C.; Watson, J.G.; Sloane, C.S. "An Overview of the 1987-1988 Metro Denver Brown Cloud Study," In *Visibility and Fine Particles*; Mathai, C.V., Ed.; TR-17, A&WMA, Pittsburgh, PA, 1990; pp 363-373.

This paper presents an overview of the design and methods used in the 1987-1988 Metro Denver Brown Cloud Study and a summary of the study results. The objectives of the study were to quantify the effect on extinction (particularly due to sulfates) when metro area coal-fired power plants were switched to natural gas, and to determine the contribution of all major sources to light extinction. In addition to fine particle, gaseous, visibility, and meteorological measurements, source characterization tests were performed to establish area-specific chemical source profiles. Categories included in the source apportionment included clean air, NO₂, primary geological material, primary boilers, primary mobile source exhaust, primary woodburning, secondary ammonium sulfate, and secondary ammonium nitrate. Extinction efficiencies were estimated for sulfate, nitrate, elemental carbon, and organic carbon using linear regression and deterministic calculations. Source apportionment was determined by receptor modeling, using the chemical mass balance (CMB) model.

Approximately one-third of the NO_x emissions are from mobile sources, one-third from power plants, and the rest from space heating and other sources. Approximately 70% of the area's SO₂ emissions are from coal-fired power plants. Other sources include a brewery, refineries, and diesel engines. Although an ammonia emissions inventory has not been developed for the Denver area, it is likely that agricultural and biogenic sources are significant.

Organic and elemental carbon combined were the largest contributors to fine-particle mass (<2.5 μm), accounting for approximately 50% of the fine-particle mass. Nitrates accounted for 20% of the fine-particle mass and sulfate and ammonium each contributed approximately 8%. Sampling artifacts may have resulted in an overestimation of 15% in the organic carbon concentration and a 10%-20% underestimation of the nitrate concentration. On the average, 50%-60% of the light scattering was due to particle scattering, 24%-28% to particle absorption, 7%-12% to gas absorption, and 6%-8% to gas scattering. Elemental carbon had the largest light extinction efficiency (9.1 m²/g at 50% RH). The extinction efficiency of ammonium sulfate was 4.3 m²/g, and ammonium nitrate and organic carbon each had extinction efficiencies of 3.6 m²/g. The extinction efficiencies of organic carbon, ammonium nitrate, and ammonium sulfate are humidity-dependent and increase by over 30% at high relative humidities (>80% RH). The light-extinction efficiency was 1.0 m²/g for geological dust and primary boiler emissions (fly ash) and 0.17 m²/g for NO₂.

Fuel switching at metro area power plants occurred whenever a clearing of air pollution was predicted after storms or periods of high winds. Emissions inventory estimates indicated that SO₂ emissions were reduced by approximately 70%, and NO_x emissions were reduced by at least 10% during gas-burning periods. The reduction in SO₂ emissions as a result of fuel switching from coal to natural gas produced a proportional reduction in ambient SO₂ levels; however, a proportional reduction in ambient sulfate levels did not occur. Although the maximum extinction attributed to sulfates during coal- and gas-burning periods was 54 ± 17 Mm⁻¹ and 26 ± 8 Mm⁻¹, respectively, the differences were not measured over the entire study. Due to differences in meteorological conditions during coal- and gas- burning periods, it was not possible to evaluate the

impact of the two fuels on visibility unambiguously. Meteorological conditions associated with severe pollution episodes occurred more frequently during gas-burning periods. Also, emissions from a distant coal-fired power plant may have contributed to the sulfate levels measured during gas-burning periods.

Dietrich, D.L.; Molenaar, J.V.; Faust, J.F.; Watson, J.G. "Transmissometer Extinction Measurements in an Urban Environment," In *Visibility and Fine Particles*; Mathai, C.V., Ed.; TR-17, A&WMA, Pittsburgh, PA, 1990; pp 374-383.

This paper describes the design, implementation, and operational application of the Optec LPV-2 long-range transmissometer which was used to continuously monitor the total light extinction during the 1987-1988 Metro Denver Brown Cloud Study. The extinction was measured along a 2.67-km sight path, 75 m above street level (midlevel of the haze layer during daylight hours) in downtown Denver. Total extinction is usually estimated from point measurements of light scattering and absorption by particles and gases. Direct measurements of total extinction with the Optec LPV-2 transmissometer compared favorably with two methods of estimating total extinction (from collocated independent point measurements), with correlation coefficients of approximately 0.9. The median extinction for the study period was 81 Mm^{-1} (standard visual range, SVR, of 48 km); however, hourly and daily extinction varied over a wide range. During a classic 5-day winter haze event, total extinction ranged from approximately 50 to 700 Mm^{-1} (SVR of 78 to 6 km). Total extinction ranged from 25 to 100 Mm^{-1} (SVR of 150 to 39 km) during periods which were relatively pollutant free. The Colorado Air Quality Control Commission adopted an extinction visibility standard of 76 Mm^{-1} (SVR of 51.5 km or 32 mi) based on the results of the study. If the extinction for a four-hour average anytime between 8 a.m. and 4 p.m. is greater than this standard, a high-pollution day is declared by the Colorado Department of Health. An Optec transmissometer was installed in Denver in January 1990 for measuring extinction relative to the standard.

"EPA Issues Final Rule Designed to Improve Visibility in Grand Canyon," *Journal of the Air and Waste Management Association* 1991, 41, 1496.

On September 18, 1991, the EPA issued a final rule consistent with an agreement reached between the Salt River Project (SRP) and several environmental groups headed by the Grand Canyon Trust and the Environmental Defense Fund and facilitated by the EPA, that will significantly reduce air pollution and improve visibility in the Grand Canyon. Under the rule, SO_2 emissions from the SRP-operated 2250-MW coal-fired Navajo Generating Station (NGS), one of the largest electric utilities in the country, will be reduced 90%. The haze in the Grand Canyon typically occurs in 2-5 day episodes and consists of a bright white layer with a distinct upper edge and occasionally one or more perceptible layers. The visibility impairment in the Grand Canyon is caused by a mixture of nitrates, sulfates, and dust particles. A 300% improvement in visibility is expected during the worst haze episodes and a greater than 7% average improvement is expected over the winter months (November-March) when there are increasing numbers of visitors to the Canyon. In 1989, approximately 900,000 people visited the Canyon in the winter, 21% of the annual total.

In February 1991, the EPA initially proposed a 0.30 lb per million Btu SO₂ emission limit for the NGS, a 70% reduction from currently allowable SO₂ emission levels. Under the rule issued in September, the emission limit was set at 0.10 lb of SO₂ per million Btu or a 90% reduction from current levels. The NGS will also shut down some of its units for maintenance during the winter months, when plant emissions contribute most to visibility impairment. Thus, the final rule provides tougher control at a lower cost than EPA's proposal, \$430 million instead of \$510 million. The levelized annual cost based on flue gas desulfurization using wet scrubbers, which the EPA considers the best control technology currently available, is \$90 million (1992 dollars). The controls will be phased in from 1997 to 1999.

Federal Register 1990, 55, 38403-38408.

The Department of the Interior has determined that the increase in emissions resulting from a proposed electric generating station by Multitrade Limited and other proposed facilities in Virginia is very likely to worsen the existing adverse visibility conditions at Shenandoah National Park and cause further perceptible visibility degradation. Therefore, it has recommended that the Virginia Department of Air Pollution Control deny a permit to Multitrade Limited for a major new emitting facility 110 km southwest of the park unless measures are taken to ensure that the proposed source will not contribute to adverse impacts on park resources.

As of September 1990, the Virginia Department of Air Pollution Control had recently granted permits for the construction and operation of four electric generating facilities, and applications for eleven other proposed facilities were in the review process. All fifteen of the facilities are within 200 km of Shenandoah National Park. The four permitted facilities have estimated SO₂, NO_x, and VOC emissions of 5988, 9512, and 475 tons per year, respectively. The estimated SO₂, NO_x, and VOC emissions from the other eleven proposed facilities (including Multitrade Limited) are 14,101, 26,792, and 115 tons per year, respectively. If all fifteen facilities were constructed and operated as proposed, statewide emissions of SO₂ and NO_x would increase by 7% and 22%, respectively, with even larger percentage increases in the vicinity of the park. Data from the Virginia Department of Air Pollution Control indicate that SO₂ and NO_x emissions would increase by 37% and 113%, respectively, for all point sources within approximately 100 km of the park boundary.

The estimated visual range in the eastern United States under natural conditions, without the influence of air pollution, is 150 ±45 km based on studies of historic visibility conditions. Sulfur has dominated the haziness over the eastern United States since the late 1940's. The estimated natural fine-particulate mass and natural sulfate concentrations in the East are 3.3 μg/m³ and 0.2 μg/m³, respectively. The annual average visibility in the southeastern United States declined 60% from 1948 to 1983, with a decline of 40% in the winter and 80% in the summer. The average visual range in rural areas of the East is currently 20-35 km, significantly less than the estimated visual range of 150 km under natural conditions. Sulfates are currently responsible for most of the visibility impairment in the East.

The National Park Service (NPS) has been monitoring visibility at the park since 1980. Data collected in 1988 and 1989 show that during the summer (June-September) the monthly average fine-particle concentration ranged from 19.5-28.9 $\mu\text{g}/\text{m}^3$, six to nine times higher than the estimated annual average natural background concentration. From June 1982 to May 1986, the summer average fine-particle mass concentration was 16 $\mu\text{g}/\text{m}^3$, five times the estimated natural background. The average concentration for the entire period was 10 $\mu\text{g}/\text{m}^3$, three times the estimated natural background.

Researchers have shown that sulfates are responsible for 70%-85% of the visibility impairment at Shenandoah National Park. The average summer sulfate concentration between 1982 and 1984 ranged from 8.5-10.2 $\mu\text{g}/\text{m}^3$, forty to fifty times the natural background. The annual average sulfate concentration between 1982 and 1986 was 5.8 $\mu\text{g}/\text{m}^3$, nearly thirty times higher than the natural background concentration. In the summer of 1989, the average sulfate concentration was 11.2 $\mu\text{g}/\text{m}^3$, and the 12-month average for Dec. 1988-Nov. 1989 was 6.4 $\mu\text{g}/\text{m}^3$. Organics are responsible for most of the remaining visibility impairment. Nitrate aerosols average less than 2 $\mu\text{g}/\text{m}^3$ and are typically responsible for less than 1% of the visibility impairment. Occasionally, nitrates make up 10%-20% of the fine particle mass and may significantly affect visibility.

The NPS visibility monitoring program has shown that, with respect to uniform haze, visibility at Shenandoah National Park is impaired by anthropogenic pollution 90% of the time. In fact, visitor surveys have shown that poor visibility is the single most frequent complaint by visitors to the park. Studies on human perception of visual air quality have shown that a 5% change in extinction (standard visual range) is the lower-bound threshold which would be noticeable by a sensitive observer. A 15% change in extinction represents the upper-bound threshold which should be noticed by a casual observer.

Teleradiometer (1980-1987) and transmissometer (since 1989) measurements show that the median visual range at the Shenandoah National Park ranges from 10-113 km, with a geometric mean (1987) of 65 km. Therefore, median visibility at the park is one-tenth to three-fourths of the estimated natural visual range of 150 km, with an average visibility approximately 40% of natural conditions on an annual basis. Visibility in the park exhibits a seasonal pattern, with the worst visibility in the summer when park visitation is highest. The average visibility in the summer months ranges from 10-36 km, less than one-fourth of the estimated natural visual range.

Research by the NPS has shown that both local (within 200 km) and long-distance sources contribute to the uniform haze at Shenandoah National Park. Source areas in Ohio, Kentucky, West Virginia, Indiana, Michigan, and Illinois, in addition to Virginia, have been estimated to contribute to the visibility impairment at the park under certain conditions.

Prior to the passage of the Clean Air Act Amendments, the EPA had estimated that SO_2 emissions in Virginia would more than double by 2010. The Clean Air Act Amendments are expected to result in a reduction in sulfur dioxide emissions of almost 50% in the eastern United States;

however, the EPA estimates that SO₂ emissions will continue to increase in Virginia despite the overall reduction in the East, particularly between now and 2005. The Department of the Interior has suggested that Virginia develop a statewide emissions control strategy to protect the air quality related values in Shenandoah National Park, including an offset program requiring greater than one-for-one emissions reductions elsewhere in the state to offset proposed emission increases from major new or modified sources. The emissions control strategy would also establish a time frame for determining maximum allowable levels of air pollution in the state (statewide emission caps).

Federal Register 1992, 57, 4465-4470.

Studies by the National Park Service (NPS) have shown that air pollution is adversely impacting visibility and other air quality related values (AQRVs) at Great Smoky Mountains National Park. Therefore, the Department of the Interior has recommended that the Tennessee Air Pollution Control Division, as well as permitting authorities in North Carolina, South Carolina, and Georgia, deny permits for major new sources within 200 km of the park unless steps are taken to ensure that these sources do not contribute to adverse impacts on the park. The Interior Department has recommended the development of an emissions control strategy to protect the AQRVs of Great Smoky Mountains National Park including greater than one-for-one emissions reductions elsewhere in the state to offset proposed emission increases from major new sources and a statewide Reasonable Available Control Technology requirement to control emissions from existing sources. The emissions control strategy would also include a provision setting a time frame for determining maximum allowable levels of air pollutants in the state. Statewide emissions caps would be the primary vehicle for achieving the maximum allowable levels. Separate action is currently pending on a proposed new boiler at the Tennessee Eastman facility in Kingsport, TN, which would increase NO_x emissions in the area by 1542 tons per year. Sampling by the NPS has shown that Great Smoky Mountains National Park receives the highest nitrate deposition of any monitored national park.

The estimated visual range in the eastern United States under natural conditions, without the influence of air pollution, is 150 ± 45 km based on studies of historic visibility conditions. Sulfur has dominated the haziness over the eastern United States since the late 1940's. The estimated natural fine-particulate mass and natural sulfate concentrations in the East are 3.3 µg/m³ and 0.2 µg/m³, respectively. The annual average visibility in the southeastern United States declined 60% from 1948 to 1983, with a decline of 40% in the winter and 80% in the summer. The average visual range in rural areas of the East is currently 20-35 km, significantly less than the estimated visual range of 150 km under natural conditions. Sulfates are currently responsible for most of the visibility impairment in the East.

The NPS has been monitoring visibility at Great Smoky Mountains National Park since 1984, initially using cameras and teleradiometers to determine visual range. From 1985 through 1987, fine-particulate samples were collected using stacked filter units (SFU). Since 1988, visibility at the park has been monitored as part of EPA's IMPROVE sampling network for class I areas. The visibility monitoring program has shown that,

with respect to uniform haze, visibility at Great Smoky Mountains National Park is impaired by anthropogenic pollution greater than 90% of the time, with sulfates responsible for 70%-85% of the visibility impairment. Organics are responsible for most of the remaining visibility impairment. Nitrate aerosols are typically responsible for less than 1% of the visibility impairment, with an average concentration of less than $3 \mu\text{g}/\text{m}^3$. On occasion nitrates comprise up to 10% of the fine-particle mass and may have a significant impact on visibility. Research by the NPS has shown that, in addition to local sources (those within 200 km), source areas in Ohio, Kentucky, West Virginia, Virginia, Indiana, North Carolina, and Illinois may also contribute to the haze obscuring the scenic views in the park.

The summer (June-September) average fine-particle concentration measured at the park from March 1988 to February 1991 using the IMPROVE sampler ranged from 8.7 to $25.1 \mu\text{g}/\text{m}^3$, three to eight times higher than the estimated annual average natural background concentration. Data obtained during the period from March 1985 to February 1987 using the SFU showed that the average summer fine-particle mass concentration was $9.3 \mu\text{g}/\text{m}^3$, three times the estimated natural background. The average fine-mass concentration for the entire period was $6.4 \mu\text{g}/\text{m}^3$, twice the estimated natural background. Analysis of the SFU data showed that the average summer sulfate concentration between 1985 and 1987 ranged from 1.9 - $8.3 \mu\text{g}/\text{m}^3$, ten to forty-two times the natural background concentration. The average annual sulfate concentration over the 1985-1987 time period was $4.9 \mu\text{g}/\text{m}^3$, almost twenty-five times higher than the natural background. The IMPROVE data were slightly higher than, but consistent with, the SFU data. The IMPROVE data show that the average summer sulfate concentration from 1988 to 1990 was $9.4 \mu\text{g}/\text{m}^3$, and the average sulfate concentration from March 1988 through February 1991 was $5.7 \mu\text{g}/\text{m}^3$.

The median visual range at Great Smoky Mountains National Park is 39 km, with a median summertime visual range of 19 km. Thus, visibility at the park has decreased to less than one-fourth of the estimated natural visual range. Visibility conditions at the park are strongly dependent on the season, with the worst visibility in the summer when park visitation is the highest. The average visibility in the summertime ranges from 23-43 km, which is less than one-third of the estimated natural visual range.

Flocchini, R.G.; Cahill, T.A.; Eldred, R.A.; Feeney, P.J. "Particulate Sampling in the Northeast: A Description of the Northeast States for Coordinated Air Use Management (NESCAUM) Network," In *Visibility and Fine Particles*; Mathai, C.V., Ed.; TR-17, A&WMA, Pittsburgh, PA, 1990; pp 197-206.

A description of the Northeast States for Coordinated Air Use Management (NESCAUM) sampling network is presented. The NESCAUM network consists of seven regionally representative rural sites in eight states from Maine to New Jersey. The objective of the network is to define regional patterns of ambient fine-particulate matter.

Hameed, S.; Dignon, J. "Global Emissions of Nitrogen and Sulfur Oxides in Fossil Fuel Combustion 1970-1986," *Journal of the Air and Waste Management Association* 1992, 42, 159-163.

Estimates of global NO_x and SO_x emissions due to fossil fuel combustion are presented on a year by year basis from 1970 to 1986. The estimates are based on statistical models of the relationships between emissions and rates of fuel consumption. Nitrogen oxide emissions varied linearly with total fuel consumption and SO_x emissions exhibited a bilinear dependence on the rates of consumption of solid and liquid fuels. Estimates of the geographical distribution of NO_x and SO_x emissions for 1986 are presented on a latitude-longitude grid (with a resolution of 4.5° in latitude and 7.5° in longitude) which are suitable for use in global circulation models for three-dimensional simulations of atmospheric chemistry.

Emissions of total global NO_x increased by one-third, from 18 million tons N in 1970 to 24 million tons N in 1986. The average rate of increase from 1970 to 1986 was 1.8% per year, which is less than the historical rate of increase of 3.4% per year. Global NO_x emissions remained steady from 1977 to 1982 due to decreasing emissions in Europe and North America which offset increasing emissions in Asia and the USSR. In 1986, the five largest emitters of NO_x , in order, were the U.S., USSR, China, Japan, and West Germany. NO_x emissions in the United States peaked in 1979 and declined during the 1980s.

Global emissions of SO_x increased by approximately 18%, from 57 million tons S in 1970 to 67 million tons S in 1986. Emissions of SO_x declined steadily from 1973, excluding small increases in 1977 and 1984. European emissions fluctuated, with 1986 emissions nearly the same as in 1970. Asian emissions nearly doubled between 1975 and 1986, due primarily to an increased use of coal combustion in China, where the largest percent increase in SO_x emissions occurred (67%). Sulfur oxide emissions in China increased from 6 million tons S in 1970 to 10 million tons S in 1986. The five largest emitters of SO_x in 1986 were the USSR, U.S., China, India, and Poland.

Hanson, D. "Haze Obscuring Grand Canyon to be Reduced," *Chemical and Engineering News* 1991, 69, 7.

An agreement that should reduce the haze obscuring the view at the Grand Canyon has been reached by the Grand Canyon Trust, a conservation group, and the Salt River Project (SRP), an Arizona public utility and operator of the 2250-MW coal-fired Navajo Generating Station (NGS). Studies by the EPA in the 1980s and by the utility itself in 1990 showed that 40% to 60% of the sulfur dioxide in the fine particulates during the worst haze episodes came from the NGS. The Grand Canyon is the only area where the EPA has been looking at visibility standards. Therefore, this is the first, and probably only, time the EPA will act solely to protect visibility in a national park.

In February 1991, the EPA proposed a 70% reduction in SO_2 emissions at a cost of \$106 million a year. Under the new EPA-approved agreement, emissions will be reduced 90% at an annual cost of \$90 million. The savings result from changing the way in which the averaging time is

calculated for meeting the lower emissions level. The EPA-proposed plan used a 30-day averaging time which would have required extensive backup equipment. The new plan uses an annual rolling average, cutting the equipment cost 30%. The plant currently emits approximately 1 lb of SO₂ per million Btu. This will be reduced to 0.1 lb of SO₂ per million Btu using wet scrubbers. By 1999, when the controls are fully in place, the annual levelized cost could be reduced by more than \$35 million/yr through the sale of credits for the removal of 63,000 tons/yr of SO₂ earned under the revised Clean Air Act's SO₂ allowance-trading program. The credits should be worth approximately \$570 per ton of SO₂.

Miller, D.F.; Flores, M. "Sulfur Dioxide Concentrations in Western U.S.," *Atmospheric Environment* 1992, 26A, 345-347.

Weekly integrated SO₂ concentrations are presented for national parks in the western U.S., northern Minnesota, Alaska, and Hawaii for the period November 1986 to October 1987. The highest and most variable concentrations were measured at Hawaii Volcanoes National Park due to the activity of the Kilauea Volcano. Concentrations varied from 0.04 $\mu\text{g m}^{-3}$ (the minimum detection level) to 179 $\mu\text{g m}^{-3}$, with an annual mean SO₂ concentration of 30 $\mu\text{g m}^{-3}$. The SO₂ concentrations in Voyagers National Park, MN, and the five parks in the western contiguous states were similar and ranged from 0.83 to 1.64 $\mu\text{g m}^{-3}$; the grand mean was 1.3 $\mu\text{g m}^{-3}$. The SO₂ concentration typically ranges from 0.1 to 0.15 $\mu\text{g m}^{-3}$ over the Pacific Ocean and from 5 to 50 $\mu\text{g m}^{-3}$ in the eastern United States.

Novakov, T.; Chang, S.G.; Harker, A.B. "Sulfates as Pollution Particulates: Catalytic Formation on Carbon (Soot) Particles," *Science* 1974, 186, 259-261.

This paper describes laboratory experiments on the gas-solid reaction of SO₂ with carbon. Electron spectroscopy for chemical analysis (ESCA) confirmed that both graphite and soot particles oxidize SO₂ in air. More sulfate was produced when the soot was exposed to humidified air than when it was exposed to dry air. Only low, background level peaks were produced when dry and humidified N₂ was used. The experiments also showed that soot-catalyzed oxidation of SO₂ occurred in the presence of flames and combustion-produced gases.

They also found a correlation between ambient concentrations of carbon and SO₄²⁻ in Los Angeles, which supports their hypothesis that carbon (soot) oxidation may be an important pathway for sulfate formation. The catalytic formation of sulfate on soot particles may be of greatest significance in the open atmosphere, particularly near combustion sources, where the concentrations of SO₂ and soot are highest.

Ondov, J.M.; Kelly, W.R. "Tracing Aerosol Pollutants with Rare Earth Isotopes," *Analytical Chemistry* 1991, 63, 691A-697A.

The authors describe the use of enriched stable isotopes of rare-earth elements to definitively track the movement of fine particles emitted from a specific source (or sources) and to determine how much material is deposited at a particular location. Enriched rare-earth tracers are applicable in the study of dry particle deposition and other

atmospheric phenomena. Enriched isotopes of Sm have recently been used in an EPA study to determine the contributions of residual heating oil combustion and diesel motor vehicles to airborne mutagens.

Particulate tracers with the power of inert gas tracers (such as deuterated methane and perfluorocarbon tracers used to study plume dispersion and transport) are essential in the study of the role SO₂, NO_x, and particulates and the secondary aerosols formed from them play in the atmosphere. Enriched stable rare-earth elements are well-suited as particulate tracers because they are nontoxic, chemically stable, nonradioactive, and relatively inexpensive. They can withstand high-temperature combustion environments and are detectable with an ultimate sensitivity of 1 part in 10¹⁵ (mass of tracer to mass of air).

Rare-earth isotopes are particularly useful because the relative abundances of most rare-earth isotopes are nearly constant in nature and can be measured with great precision by thermal ionization mass spectrometry (TIMS). Therefore, instead of elevating the atmospheric concentration of the rare-earth element by an amount suitably in excess of its variability, it is only necessary to perturb the abundance ratio. Because the natural isotopic ratios are invariant, temporal or spatial biases arising from variations in the background concentration of the tracer element in the aerosol and reagents used in the analysis are eliminated. For example, neodymium has seven stable isotopes ranging in mass from 142 to 150. The background concentration of naturally occurring Nd can be determined simply by measuring one of the six other unperturbed Nd isotopes. In addition, several sources can be tagged simultaneously, each with a different isotope, and the relative and absolute contributions of each source can be determined in a single sample by its unique isotopic signature.

Application of the technique involves injecting enriched isotopes of rare-earth elements into the flue gas or fuel of a high-temperature combustion source and then measuring the perturbations of the natural isotopic ratios in aerosol particles collected in airsheds influenced by the source. Preliminary calculations using a multicomponent aerosol dynamics computer code, MAEROS, suggested that tracer particles <10 nm in diameter would be needed for quantitative scavenging by power plant particles under conditions expected in typical coal-fired power plants. Various particle generation techniques, including air-atomizing nozzles and a condensation technique were tested and optimized in the laboratory, and then field-tested at a small coal-fired utility boiler to determine if the tracer was actually becoming attached to the fly ash particles. In the field test, the tracer was injected near the inside wall of the duct work at the outlet of an air preheater. Despite passing through an induced-draft fan with a large reduction in volume, the tracer did not become well-mixed throughout the duct. Therefore, interpretation of the data was difficult because tagged fly ash was mixed with untagged fly ash and unattached tracer particles at the sampling location.

A technique was developed in which the 2,2,6,6-tetramethyl-3,5-heptanedione chelates of enriched Nd isotopes were vaporized and then degraded in the presence of fly ash. This technique delivered approximately 70 times more tracer than using a single nozzle atomizer. The vaporization technique was used to release ¹⁴⁹Nd in an urban-scale

test outside Washington, D.C. Aerosol samples were collected at 13 sites along a 72° arc located 20 km from a 100-MW coal-fired utility boiler. The tests were successful in that the signal-to-noise ratios were in good agreement with predictions for various particle size ranges. Measured tracer concentrations in ambient air agreed (within a factor of 3) with concentrations estimated from the release rate and plume dispersion calculations, except for 2 sites where sample contamination occurred.

Richards, L.W.; Anderson, J.A.; Blumenthal, D.L.; McDonald, J.A.; Bhardwaja, P.S.; Candelaria, R.B.; Moon, D.W. "Nitrogen and Sulfur Chemistry and Aerosol Formation in a Western Coal-Fired Power Plant Plume," In *Visibility and Fine Particles*; Mathai, C.V., Ed.; TR-17, A&WMA, Pittsburgh, PA, 1990; pp 242-259.

Results are presented from airborne sampling in the vicinity of the Navajo Generating Station (NGS) at Page, Arizona, during the August 1980 Source Emission and Plume Characterization (SEAPC) Study. The SEAPC Study was conducted to obtain measurements of the rate of formation of sulfate and light-scattering particles in the NGS plume over a range of relative humidities. Plume chemistry, aerosol, and plume dispersion data were collected at distances of up to 140 km from the power plant.

The SEAPC study complements data obtained from the 1979 EPA/SRP (Salt River Project) sponsored Visibility Impairment due to Sulfur Transport and Transformation in the Atmosphere (VISTTA) Studies. The VISTTA data were obtained during periods of low relative humidity. During the VISTTA Study, the sulfate formation rates were about ten times smaller than expected and the secondary particles produced were too small to scatter light effectively. Aerosol formation was delayed until the emitted nitric oxide (NO) was oxidized to nitrogen dioxide (NO₂) by the ozone in the background air. EPA review of existing data on the formation of sulfate in plumes indicated that the VISTTA data were outliers. Another unusual result from the VISTTA Study was that essentially no fine-particle sulfate was emitted by NGS. Typically, sulfate formation is delayed until the plume is quite dilute. Thus, due to the emphasis on measurement of the optical properties of the NGS plume near the source during VISTTA, very few data points were obtained for sulfate and aerosol formation in the NGS plume under summertime conditions at distances where sulfate would likely form.

Results from SEAPC indicated that the NGS plume usually remained concentrated enough at distances of 50 km or more to contain significant amounts of NO which had not yet been converted to NO₂ by the background ozone. The authors believe that the persistence of unreacted NO and the accompanying depression of the ozone concentration contributed significantly to the slow initial oxidation rates for NO₂ and sulfur dioxide. Nitric acid was formed in the plume, but particulate nitrate was not. The ammonia gas concentration was so small that the nitric acid formed in the plume was not concentrated enough to saturate the plume with respect to the formation of solid ammonium nitrate. On the average, ammonium concentrations were 60% of those necessary to completely neutralize the sulfate and nitrate in the aerosol.

Size distributions were determined for both the primary aerosol (fly ash) and secondary aerosol (sulfates formed in the plume). On the day

with the lowest relative humidity (21%) during the study, the plume aerosol size distribution showed little or no formation of secondary (accumulation mode) aerosol; however, the primary (fly ash) emissions were clearly evident in the size range larger than approximately $0.5 \mu\text{m}$. On a day when the relative humidity was 83% at the start of the flight and averaged 77% during the sampling pass, formation of secondary aerosol was greatly accelerated. The secondary aerosol formed under conditions of higher humidity was capable of scattering light more effectively than sulfate formed at lower humidities.

Results from SEAPC indicated that conversions of SO_2 to sulfate were typically only a few percent; for example, at a distance of 140 km only 6.4% of the sulfur dioxide was converted to sulfate. As shown by VISTTA, little formation of sulfate, nitrate, and light-scattering aerosol occurred during the first 70 km of plume travel. The largest sulfate formation rate observed in SEAPC was 1.6% per hour, which is only about one-third as large as typically observed in other studies. In the daytime, NO_x was oxidized to nitric acid approximately five times faster than SO_2 was oxidized to sulfate at low to moderate relative humidities in the dilute plume. It is believed that sulfate formation is very slow at night; however, nitrate formation occurs in the dark at an appreciable rate (in the presence of ozone). Ozone and NO_2 react to form NO_3 , and then N_2O_5 , which is hydrolyzed to nitric acid. These reactions do not occur at night because NO_3 is both photolyzed and destroyed by NO .

Robinson, E.; Robbins, R.C. "Gaseous Sulfur Pollutants from Urban and Natural Sources," *Journal of the Air Pollution Control Association* 1970, 20, 233-235.

Estimates of natural and anthropogenic sulfur emissions are presented, along with a discussion of scavenging processes. Natural sources of sulfur emissions are sulfate aerosols produced in sea spray and H_2S from the decomposition of organic matter and minor amounts from volcanic activity. Sulfur dioxide emissions are almost exclusively of anthropogenic origin. The total estimated annual emissions of SO_2 based on 1965 world data were 146 million tons. Of the SO_2 emissions, 70% resulted from coal combustion, 16% from the combustion of petroleum products (mainly residual fuel oil), and the remainder from petroleum refining and nonferrous smelting. Sources in the northern hemisphere were responsible for 93% of the total SO_2 emissions. Emissions of SO_2 were 69 million and 78 million tons in 1937 and 1940, respectively. Thus worldwide emissions of SO_2 nearly doubled between 1940 and 1965.

Hydrogen sulfide is rapidly oxidized to SO_2 in the troposphere by heterogeneous reaction on aerosol particles. The lifetime of H_2S ranges from approximately two hours in urban areas to two days in remote unpolluted areas. The solubility of SO_2 in water droplets with low pH is small; however, the aqueous oxidation of SO_2 may be promoted by the absorption of ammonia from the atmosphere which neutralizes the acid formed. A significant scavenging mechanism for SO_2 is the photochemical oxidation of SO_2 in mixtures with NO_2 and hydrocarbons. Once SO_2 and H_2S are in aerosol form as SO_4 , precipitation scavenging by clouds and rain is an effective removal process. Sulfur dioxide is also scavenged from the atmosphere by vegetation. The deposition velocity of SO_2 calculated from chamber studies is approximately 1 cm/sec.

Background concentrations of H₂S, SO₂, and SO₄ were estimated from measurements in remote areas and used to estimate the environmental sulfur cycle (based on available data) which indicates a net transfer of sulfur from land to ocean areas. Estimates of the background concentration of SO₂ range from less than 0.3 ppb to 1 ppb. The background SO₄ concentration was estimated at 2 μg/m³.

Sloane, C.S.; Watson, J.G.; Chow, J.C.; Pritchett, L.; Richards, L.W. "Size Distribution and Optical Properties of the Denver Brown Cloud," In *Visibility and Fine Particles*; Mathai, C.V., Ed.; TR-17, A&WMA, Pittsburgh, PA, 1990; pp 384-393.

The Micro-Orifice Uniform Deposit Impactor (MOUDI) was used to determine mass as a function of particle size (eight size ranges less than 1.8 μm) for sulfate, nitrate, organic and elemental carbon during the 1987-1988 Denver Brown Cloud Study. Particulate mass was also simultaneously measured using teflon membrane and quartz fiber filters in a modified sequential filter sampler (SFS). The two methods of measurement were in good agreement for sulfate, nitrate, total carbon, and fine-particle mass. Comparison of the MOUDI and SFS organic carbon measurements indicated that the organic carbon measurements from the SFS quartz fiber filters were substantially positively biased. Analysis of fresh and aged fine-particle modes indicated that agricultural emissions of ammonia from areas northeast of Denver contribute significantly to the formation of fine ammonium nitrate in Denver. However, the small number of measurements from genuine episodes of visibility impairment, and the lack of a thorough ammonia emissions inventory for the Denver airshed, prevent a conclusive determination of the degree ammonia emissions control the formation of fine ammonium nitrate in Denver.

Sulfate had the largest light-scattering efficiency, followed by nitrate and organic carbon. The light-scattering efficiency of soot (elemental carbon) was much lower than that of the other chemical constituents. However, elemental carbon is much more efficient at light-absorption than the other principal species. The authors concluded that meteorological conditions that produce episodes of visibility impairment in Denver can be distinguished by the associated fine-particle-size distributions. Thus the light-scattering efficiencies of the principal chemical constituents are not constants.

"Smoky Mountains: More Controls Needed," *Air and Water Pollution Control* 1992, 5, 8.

Visibility impairment and other air pollution-related problems in the Great Smoky Mountains National Park have resulted in a recommendation by the Interior Department that new permit applications for air pollution sources near the park be denied. The Department has recommended that the Tennessee Air Pollution Control Division, as well as air permitting authorities in North Carolina, South Carolina, and Georgia, deny permits for major new sources within approximately 200 km (120 miles) of the park unless steps are taken to prevent further impacts on the park. Studies by the Interior Department have shown that fine particulate concentrations in the Smoky Mountains are three to eight times higher than the estimated annual summer natural background concentration. The Interior Department suggested that the states surrounding the park

develop an emissions control strategy, which might include greater than one-for-one emissions reductions elsewhere in the region to offset proposed increases in the area near the park.

The recommendation cannot, by itself, stop the issuance of permits; the final decision rests with the appropriate state agencies. Despite the same recommendation by the Interior Department in September 1990 for the Shenandoah National Park in Virginia, several new permits have been issued, and Virginia is considering a proposal for a new power plant on the edge of the park.

Thomas, J.; Parrott, H.; Yost, G. "Visibility Conditions in Eastern Wildernesses," In *Visibility and Fine Particles*; Mathai, C.V., Ed.; TR-17, A&WMA, Pittsburgh, PA, 1990; pp 343-349.

Standard visual range (SVR) data are presented for spring, summer, and fall at four wilderness areas that are part of the Eastern Region of the Forest Service: Boundary Waters Canoe Area in Minnesota; Dolly Sods Wilderness in West Virginia; Lyle Brook Wilderness in Vermont; and Great Gulf Wilderness in New Hampshire. SVRs were estimated from photographs using scanning densitometry. The objectives of the visibility monitoring are: (1) to establish a record of visibility trends in Eastern Region Class I areas, (2) to improve effectiveness in responding to visibility analysis sections in prevention of significant deterioration (PSD) permit applications, and (3) to determine if visibility impairment exists in Class I areas. The best visibility occurred at Boundary Waters Canoe Wilderness Area for all three seasons. The visibility ranged from 90-250 km on most days. The smallest SVRs occurred at Dolly Sods Wilderness Area, with median visibilities on most days between 10 and 60 km. Visibility conditions at Great Gulf and Lyle Brook Wilderness Areas were similar; however, visibility was more variable at Great Gulf. Most summer and fall days at Lyle Brook had median SVRs that ranged from 10-70 km and 80-150 km.

Wolff, G.T. "Visibility-Reducing Species in New England's Berkshire Mountains," In *Visibility Protection: Research and Policy Aspects*; Bhardwaja, P.S., Ed.; TR-10, APCA, Pittsburgh, PA, 1986; pp 453-460.

Measurements of the fine-particle composition ($<2.5 \mu\text{m}$) and light-scattering coefficient were included as part of an intensive air quality and acid deposition study in the Berkshire Mountains of western Massachusetts in the summer of 1984.

Zurer, P. "Ozone Depletion: Arctic Hole Feared; Sulfate Aerosol Blamed," *Chemical and Engineering News* 1992, 70, 4-5.

Record amounts of chlorine monoxide (ClO) were measured over Canada and northern New England during January flights of the second Airborne Arctic Stratospheric Expedition (AASE-II). Chlorine monoxide is a free radical that accelerates ozone depletion. New data, from the study, document for the first time that reactions of nitrogen oxides on sulfate aerosol particles reduce the rate at which the atmosphere can recover from chlorine-catalyzed ozone destruction. Scientists have confirmed that the subtle but accelerating loss of ozone in the mid-latitudes, as shown by satellite observations over the last decade, is catalyzed by

chlorine and bromine free radicals. The study also revealed surprisingly low amounts of nitrogen oxides. Nitrogen oxides slow the rate of ozone depletion by tying up reactive chlorine and bromine as less reactive nitrates. The observations confirm the hypothesis, which was based on laboratory observations and computer calculations, that heterogeneous reactions on sulfate aerosols use up reactive nitrogen and thus accelerate ozone loss. Measured concentrations of nitrogen oxides were low (due to reactions on aerosol particles) as far south as the mid-Caribbean.

5.0 REFERENCES

1. Weber, G.F.; Collings, M.E.; Schelkoph, G.L. "Simultaneous SO_x/NO_x Control," Final Technical Report for the Period April 1, 1987, through March 31, 1988; DE-FC21-86MC10637, Grand Forks, ND, May 1988.
2. Weber, G.F.; Collings, M.E.; Schelkoph, G.L.; Steadman, E.N. "Simultaneous SO_x/NO_x Control," Final Technical Report for the Period April 1, 1986, through March 31, 1987; DE-FC21-86MC10637, DOE/FC/10637-2414, Grand Forks, ND, April 1987.
3. Weber, G.F.; Laudal, D.L. "SO_x/NO_x Control - Catalytic Fabric Filtration for Simultaneous NO_x and Particulate Control," Final Technical Report for the Period April 1, 1988, through June 30, 1989; DE-FC21-86MC10637, Grand Forks, ND, August 1989.
4. Miller, S.J.; Laudal, D.L. "Real-Time Measurement of Respirable Particulate Emissions from a Fabric Filter," In *Particulate and Multiphase Processes, Vol. 2, Contamination Analysis and Control*; Ariman, T., Ed.; Hemisphere Pub. Corp., 1987; p 663.
5. Miller, S.J.; Laudal, D.L. "Particulate Removal Enhancement of a Fabric Filter Using Flue Gas Conditioning," Presented at the Third EPRI Conference on Fabric Filter Technology for Coal-Fired Power Plants, Scottsdale, AZ, November 19-21, 1985.
6. Laudal, D.L.; Miller, S.J. "Flue Gas Conditioning for Improved Baghouse Performance," In *Proceedings of the Sixth Symposium on the Transfer and Utilization of Particulate Control Technology*; EPRI CS-4918, November 1986, Vol. 3, p 14-1.
7. Miller, S.J.; Laudal, D.L. "Flue Gas Conditioning for Improved Fine Particle Capture in Fabric Filters: Comparative Technical and Economic Assessment," In *Low-Rank Coal Research Final Report, Vol. II, Advanced Research and Technology Development*; DOE/FC/10637-2414 (DE87006532), April 1987.
8. Miller, S.J.; Laudal, D.L. "Fine Particulate Emissions: Flue Gas Conditioning for Improved Fine Particle Capture in Fabric Filters," Final Technical Report for the Period April 1, 1987, through March 31, 1988; DE-FC21-86MC10637, Grand Forks, ND, August 1988.
9. Laudal, D.L.; Miller, S.J. "Flue Gas Conditioning for Baghouse Performance Improvement with Low-Rank Coals," In *Proceedings of the*

Fourteenth Biennial Lignite Symposium on the Technology and Utilization of Low-Rank Coals; University of North Dakota Energy and Environmental Research Center, Grand Forks, ND, 1987.

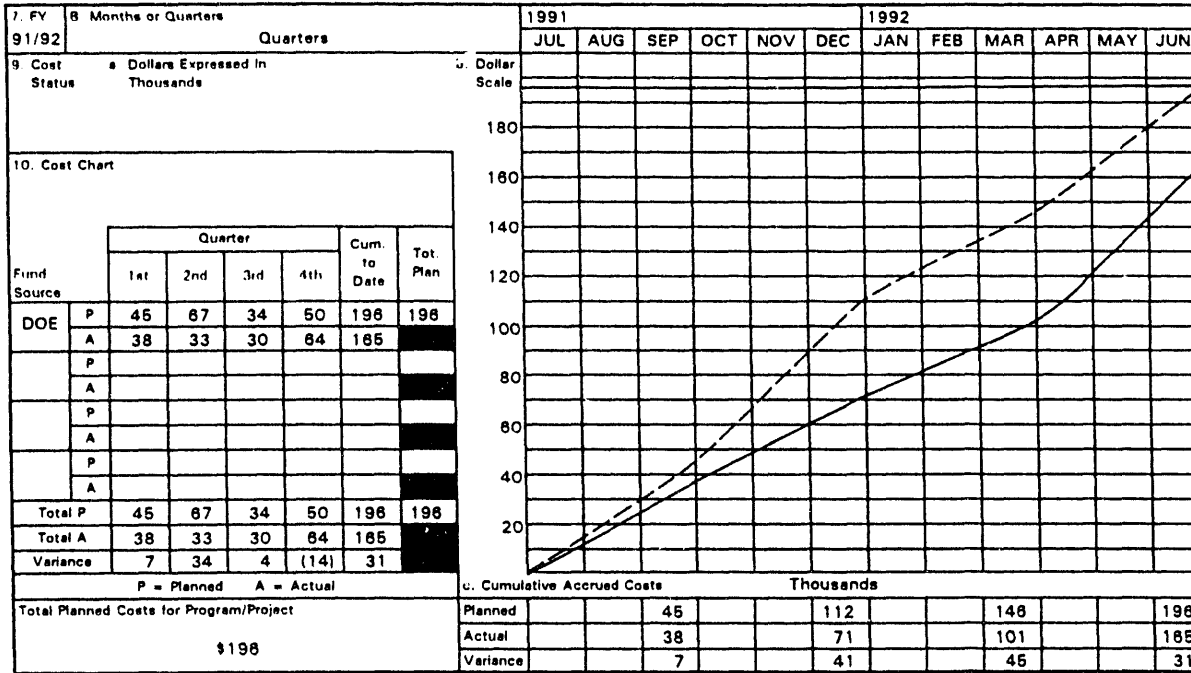
10. Miller, S.J.; Laudal, D.L.; Kim, S.S. "Mechanisms of Fabric Filter Performance Improvement with Flue Gas Conditioning," *In Proceedings of the Seventh EPA/EPRI Symposium on the Transfer and Utilization of Particulate Control Technology*; EPRI GS-6208, Vol. 2, February 1989, pp 25-1.
11. Miller, S.J. "Flue Gas Conditioning for Fabric Filter Performance Improvement," Final Project Report for Contract No. DE-AC22-88PC88866 for Pittsburgh Energy Technology Center, December 1989.
12. Miller, S.J.; Laudal, D.L. "Enhancing Baghouse Performance with Conditioning Agents: Basis, Developments, and Economics," *In Proceedings of the Eighth Particulate Control Symposium*; EPRI GS-7050, November 1990, Vol. 2, p 23-1.
13. Miller, S.J.; Laudal, D.L.; Chang, R.L. "Flue Gas Conditioning for Improving Pulse-Jet Baghouse Performance," Presented at the Ninth Particulate Control Symposium, Williamsburg, VA, October 15-18, 1991.
14. Weber, G.F.; Miller, S.J.; Laudal, D.L. "Flue Gas Cleanup," Annual Technical Project Report for the Period July 1, 1989, through June 30, 1990; DE-FC21-86MC10637, Grand Forks, ND, October 1990.
15. Weber, G.F.; Miller, S.J.; Laudal, D.L.; Heidt, M.K. "Flue Gas Cleanup," Semiannual Technical Project Report for the Period January 1, 1991, through June 30, 1991; DE-FC21-86MC10637, Grand Forks, ND, August 1991.
16. Miller, S.J.; Heidt, M.K.; Weber, G.F.; Laudal, D.L. "Flue Gas Cleanup," Semiannual Technical Project Report for the Period July 1, 1991, through December 31, 1991; DE-FC21-86MC10637, Grand Forks, ND, January 1992.
17. Groblicki, P.J.; Wolff, G.T.; Countess, R.J. "Visibility-Reducing Species in the Denver 'Brown Cloud'- I. Relationships Between Extinction and Chemical Composition," *Atmospheric Environment* 1981, 15, 2473-2484.
18. Watson, J.G.; Chow, J.C.; Pritchett, L.C.; Houck, J.A.; Burns, S.; Ragazzi, R.A. "Composite Source Profiles for Particulate Motor Vehicle Exhaust Source Apportionment in Denver, CO," *In Visibility and Fine Particles*; Mathai, C.V., Ed.; TR-17, A&WMA, Pittsburgh, PA, 1990; pp 422-436.
19. Trijonis, J.C.; Malm, W.C.; Pitchford, M.; White, W.H.; Charlson, R.; Husar, R. *Visibility: Existing and Historical Conditions--Causes and Effects*; State-of-Science/Technology Report 24, National Acid Precipitation Assessment Program 1990.
20. Hidy, G.M. "Summary of the California Aerosol Characterization Experiment," *Journal of the Air Pollution Control Association* 1975, 25, 1106-1114.

21. Trijonis, J.C. "Visibility in California," *Journal of the Air Pollution Control Association* 1982, 32, 165-169.
22. Conklin, M.H.; Cass, G.R.; Chu, L.C.; Macias, E.S. "Wintertime Carbonaceous Aerosols in Los Angeles," In *Atmospheric Aerosol-Source/Air Quality Relationships*; Macias, E.S. Hopke; P.K. Eds.; ACS Symposium Series 167, Washington, D.C., 1981.
23. Waggoner, A.P.; Weiss, R.E.; Ahlquist, N.C.; Covert, D.S.; Will, S.; Charlson, R.J. "Optical Characteristics of Atmospheric Aerosols," *Atmospheric Environment* 1981, 15, 1891-1909.
24. Covert, D.S.; Waggoner, A.P.; Weiss, R.E.; Ahlquist, N.C.; Charlson, R.J. "Atmospheric Aerosols, Humidity, and Visibility," *Advances in Environmental Science and Technology* 1980, 9, 559-581.
25. Mueller, P.K.; Henry, R.C.; Balson, W.E.; Richards, L.W.; Pitchford, M.; Watson, J.G.; Neff, W.; Saxena, P.; Wilson, W.E. "Future Research on Visibility and Fine Particles: Report from a Panel Discussion," In *Visibility and Fine Particles*; Mathai, C.V. Ed.; TR-17, A&WMA, Pittsburgh, PA, 1990; pp 972-989.
26. Porch, W.M.; Charlson, R.J.; Radke, L.F. "Atmospheric Aerosol: Does a Background Level Exist?" *Science* 1970, 170, 315-317.
27. *Air Quality Criteria for Particulate Matter and Sulfur Oxides*, Volume III; EPA-600/8-82-029c, December 1982.
28. Husar, R.B.; Holloway, J.M. "Visibility Trend at Blue Hill, ME, Since 1889," *Bulletin of the American Meteorological Society* 1981.
29. Ferman, M.A.; Wolff, G.T.; Kelly, N.A. "The Nature and Sources of Haze in the Shenandoah Valley/Blue Ridge Mountains Area," *Journal of the Air Pollution Control Association* 1981, 31, 1074-1082.
30. Neff, W.; Watson, J. "Evaluation of the Fuel-Switching Strategy Used in the Denver Brown Cloud Study," In *Visibility and Fine Particles*; Mathai, C.V., Ed.; TR-17, A&WMA, Pittsburgh, PA, 1990; pp 410-421.
31. Malm, W.C.; Iyer, H.K.; Gebhart, K. "Application of Tracer Mass Balance Regression to WHITEX Data," In *Visibility and Fine Particles*; Mathai, C.V., Ed., TR-17; A&WMA, Pittsburgh, PA, 1990; pp 806-818.
32. Latimer, D.A.; Iyer, H.K.; Malm, W.C. "Application of a Differential Mass Balance Model to Attribute Sulfate Haze in the Southwest," In *Visibility and Fine Particles*; Mathai, C.V., Ed.; TR-17, A&WMA, Pittsburgh, PA, 1990; pp 819-830.
33. Hanson, D. "Haze Obscuring Grand Canyon to be Reduced," *Chemical and Engineering News* 1991, 69, 7.
34. Seinfeld, J.H. *Atmospheric Chemistry and Physics of Air Pollution*; John Wiley & Sons, Inc.: New York, NY, 1986.

35. Novakov, T; Chang, S.G.; Harker, A.B. "Sulfates as Pollution Particulates: Catalytic Formation on Carbon (Soot) Particles," *Science* 1974, 186, 259-261.
36. Latimer, D.A.; Hogo, H. "The Relationship Between SO₂ Emissions and Regional Visibility in the Eastern United States," In Visibility Protection: Research and Policy Aspects; Bhardwaja, P.S., Ed.; TR-10, APCA, Pittsburgh, PA, 1986, pp 589-600.

U. S. DEPARTMENT OF ENERGY
FEDERAL ASSISTANCE MANAGEMENT SUMMARY REPORT

1. Program/Project Identification No DE-FC21-86MC10637	2. Program/Project Title Flue Gas Cleanup (2.1)	3. Reporting Period 4-1-92 through 6-30-92
4. Name and Address Energy and Environmental Research Center University of North Dakota Box 8213, University Station, Grand Forks, ND 58202 (701) 777-5000		5. Program/Project Start Date 4-1-88
		6. Completion Date 9-30-92



11. Major Milestone Status	Units Planned	Units Complete
A. Fine Particulate Control	P	1 ▼ 2 ▲ ▲
	C	
	P	
	C	
B. Impact of Coal Combustion on Atmospheric Visibility	P	1 ▼ 2 ▲ ▲
	C	
	P	
	C	
C. Final Project Report	P	1 ▼
	C	
	P	
	C	
	P	
	C	
	P	
	C	
	P	
	C	
	P	
	C	
	P	
	C	
	P	
	C	

12. Remarks
Due to the EERC fiscal year end, the June books do not close until July 25, 1992. Costs posted through July 8 have been included.

13. Signature of Recipient and Date <i>D. J. Miller</i> 7-31-92	14. Signature of DOE Reviewing Representative and Date
--	--

U.S. DEPARTMENT OF ENERGY
FEDERAL ASSISTANCE MANAGEMENT SUMMARY REPORT

1. Program/Project Identification No. DE-FC21-86MC10637		2. Program/Project Title Flue Gas Cleanup (2.1)		3. Reporting Period 4-1-92 through 6-30-92	
4. Name and Address Energy and Environmental Research Center University of North Dakota Box 8213, University Station Grand Forks, ND 58202 (701) 777-6000				5. Program/Project Start Date 4-1-86	
				6. Completion Date 9-30-92	
Milestone ID. No.	Description	Planned Completion Date	Actual Completion Date	Comments	
Task A	Fine Particulate Control:				
a.1	Complete reentrainment tests on pore bridging	3-31-92	6-30-92		
a.2	Complete reentrainment tests on dust surface parallel to flow	5-31-92	6-30-92		
Task B	Impact of Coal Combustion on Atmospheric Visibility:				
b.1	Complete literature review on visibility related to coal combustion	1-31-92	6-30-92		
b.2	Define approach to using particle measurement devices to predict atmospheric visibility	5-31-92	6-30-92		
Task C	Final Project Report:				
c.1	Complete Final Project Report	8-31-92			